Dose–Response Analyses of the Carcinogenic Effects of Trichloroethylene in Experimental Animals

Lorenz R. Rhomberg

Harvard Center for Risk Analysis, Harvard School of Public Health, Boston, Massachusetts USA

In lifetime bioassays, trichloroethylene (TCE, CAS No. 79-01-6) causes liver tumors in mice following gavage, liver and lung tumors in mice following inhalation, and kidney tumors in rats following gavage or inhalation. Recently developed pharmacokinetic models provide estimates of internal, target-organ doses of the TCE metabolites thought responsible for these tumor responses. Dose–response analyses following recently proposed methods for carcinogen risk assessment from the U.S. Environmental Protection Agency (U.S. EPA) are conducted on the animal tumor data using the pharmacokinetic dosimeters to derive a series of alternative projections of the potential carcinogenic potency of TCE in humans exposed to low environmental concentrations. Although mechanistic considerations suggest action of possibly nonlinear processes, dose–response shapes in the observable range of tumor incidence evince little sign of such patterns. Results depend on which of several alternative pharmacokinetic analyses are used to define target-organ doses. Human potency projections under the U.S. EPA linear method based on mouse liver tumors and internal dosimetry equal or somewhat exceed calculations based on administered dose, and projections based on mouse liver tumors exceed those from mouse lung or rat kidney tumors. Estimates of the carcinogenic potency of the two primary oxidative metabolites of TCE—trichloroacetic acid and dichloroacetic acid, which are mouse liver carcinogens in their own right—are also made, but it is not clear whether the carcinogenic potency of TCE can be quantitatively ascribed to metabolic generation of these metabolites. *Key words*: carcinogenic potency, cross-species extrapolation, dichloroacetic acid, internal dose, low-dose extrapolation, trichloroacetic acid, trichloroethylene. — *Environ Health Perspect* 108(suppl 2):343–358 (2000).
http://ehpnet1.niehs.nih.gov/docs/2000/suppl-2/343-358rhomberg/abstract.html

The U.S. Environmental Protection Agency (U.S. EPA) has in recent years produced two documents presenting its quantitative risk assessment of the carcinogenic potency of trichloroethylene (TCE) for human environmental exposures (*1,2*). Since the completion of these documents, several developments make it appropriate to revisit the question of the carcinogenic potency of TCE:

- New animal bioassays have been conducted on TCE—in particular, two gavage studies were conducted by the National Toxicology Program (NTP) (*3,4*).
- TCE pharmacokinetics and metabolism are now much better elucidated, and a good deal of work has been done on physiologically based pharmacokinetic modeling of TCE and its major metabolites in experimental animals and humans (*5–9*).
- Some of the principal metabolites of TCE are carcinogenic in their own right when directly administered to experimental animals—in particular, trichloroacetic acid (TCA) and dichloroacetic acid (DCA) cause liver tumors in mice when administered in drinking water (*10–15*).
- The understanding of the mechanisms of carcinogenic action of TCE has improved.
- The U.S. EPA has issued proposed revisions to its preferred methodology for conducting carcinogen risk assessment (*10*), which include procedures somewhat different than those used in previous agency analyses of TCE.

Many of these developments are discussed more thoroughly in the accompanying state-of-the-science articles (*6,9,16–20*) Together they raise a number of possibilities for new, more rigorous, and more biologically insightful analyses of whether and how much TCE may increase cancer risks in humans exposed to environmental concentrations.

The present article examines a number of possible approaches to dose–response analysis of the observed carcinogenicity of TCE in experimental animals together with the implications of these analyses for estimation of the low-dose potency of TCE in humans. The collection of alternative methods should be regarded as an exploration of our basis for knowing about the potential carcinogenic potency of TCE, and the credibility of each result should be influenced by informed scientific judgment, while considering the whole body of our knowledge (and the remaining uncertainties) regarding the biology and toxicology of TCE.

The end points considered for quantitative analysis are mouse liver tumors, mouse lung tumors, and rat kidney tumors. Other tumor end points have been elevated in occasional studies [e.g., lymphomas in NMRI mice (*21*), Leydig cell tumors in Sprague-Dawley rats (*22*)], but these other results have not generally been repeated and have been discussed in earlier U.S. EPA reports (*1,2*).

The proposed revision of the U.S. EPA guidelines for carcinogen risk assessment (*10*) states that biologically based dose–response models are to be preferred when sufficient data are available with which to construct reliable analyses. Although some relevant data are available, particularly in the case of mouse liver tumors, at present no such model has been developed and validated for TCE. This approach will not be considered here.

In the absence of a biologically based model, the new guidelines specify an empirical approach to dose–response analysis consisting of two alternatives designated linear and nonlinear. A choice is to be made between these on the grounds of biological understanding of the mode of action coupled with observation of the shape of the dose–response relationship in the observable region. This choice is potentially a matter of much consequence; it requires integrative interpretation of the whole body of available information and balanced consideration of the uncertainties regarding the carcinogenic modes of action of a compound as they are to be presumed to operate at low exposure levels. Rather than prejudge such decisions, which are properly considered in the risk characterization step, I have endeavored to present the key calculations for both linear and nonlinear approaches to analysis of tumor response, while examining the evidence that animal bioassay results provide regarding the shape of the dose–response relationship in the observable range.

The carcinogenic responses of test animals to TCE are believed to be ascribable not to TCE itself but to various metabolites (*16–19*). Pharmacokinetic modeling of TCE has been developing, but only recently have physiologically based models been proposed to describe the disposition and target-organ–level

This article is part of the monograph on Trichloroethylene Toxicity.

Address correspondence to L.R. Rhomberg, Gradient Corp., 238 Main St., Cambridge, MA 02142. Telephone: (617) 395-5000. Fax: (617) 395-5001. E-mail: lrhomber@gradientcorp.com

This work was supported by the U.S. Environmental Protection Agency, National Center for Environmental Assessment, under contracts T6W-0421-NATA and 8W-1278-NATA.

Received 20 October 1999; accepted 8 February 2000.

exposures of key metabolites (*5,6,8,9*). These models are used herein as a means for conducting the dose–response analyses (and projection of potential human risks from environmental exposures) on the basis of internal dosimetry. The approach employs modeled estimates of the exposure of the target organs to the metabolites that have been proposed to be responsible for their toxic reactions.

Methods

As described in the proposed revision of the U.S. EPA guidelines (*10*), empirical dose–response analysis has an initial, descriptive phase ("analysis in the range of observation") conducted by statistically fitting an appropriate dose–response model to the data to characterize the shape of the relationship in the observable region and to identify a point of departure (PoD) within this region to serve as the basis for further procedures to extrapolate to low doses.

When data on times of death of individual test animals are available, I have characterized the dose–response relationship in the observable range using the multistage-Weibull model [MULTI-WEIB (*23*), assuming incidentally discovered tumors with no time lag]. This model couples a multistage model for the effects of increasing dose with a description of the increasing incidences over time at a given dose based on an empirically determined power of time (*24*). For studies not reporting such time-to-tumor information, I use the multistage model [GLOBAL86 (*25*)] fitted to observed lifetime tumor incidence rates among bioassay animals. One rationale for the two-phase dose–response analysis in the new guidelines is that the empirical characterization of the observed dose–response patterns will not be highly model dependent within the range of observation. Nonetheless, exact calculations show minor dependencies on certain particulars of the implementation. (Studies subjected to time-to-tumor analysis were reanalyzed using the multistage model and lifetime incidences corrected for early mortality by removing data from all individuals who died before the first appearance of a tumor of interest. This cruder method for accounting for intercurrent mortality often leads to slightly higher PoD than time-to-tumor analysis, but the results do not differ appreciably.)

Although several alternatives for selecting the PoD are provided in the new guidelines proposal, the "standard point of departure, adopted as a matter of science policy" is the LED_{10} (lower [95%] statistical bound on effective dose to 10% of the population), the lower 95% confidence limit on a dose associated with 10% extra risk (*10*). Unless otherwise stated, this method of selecting the PoD is used herein. These lower limits have been calculated as provided for in GLOBAL86 (*25*) and MULTI-WEIB (*23*), i.e., they are risk-specific calculations based on reoptimizing model parameters at the 10% extra risk level. In addition, the central estimate of the dose associated with 10% extra risk, i.e., the ED_{10} (effective dose to 10% of the population), calculated based on the maximum likelihood curve, is provided. Typically, the ED_{10} is higher (and its associated low-dose slope is lower) by about a factor of 2 compared to the LED_{10}.

For the linear method, the second low-dose extrapolation phase is implemented by calculating the slope of the line segment drawn from the PoD and its risk (typically, 10% extra risk) to 0% extra risk at zero dose. This slope yields a measure of low-dose potency in terms of incremental risk per unit of dose. That is, the extrapolation invokes linearity from the PoD downward as a matter of explicitly stated policy. Since risk is taken to fall linearly from the 10% level, this low-dose slope is simply 0.1 divided by the LED_{10} (or ED_{10}). For this slope to be applied to the evaluation of human exposures, two additional steps are necessary:

- consideration of the doses (in the proffered units) that are to be presumed of equal lifetime cancer risk in the experimental animals and humans; and
- reexpression of the slope in terms of units of human exposure that are convenient for assessing environmental contamination, i.e., creating "unit risks" in terms of incremental risk per unit of continuous human exposure by ingestion, in inhaled air or in drinking water.

The first step embodies the key assumptions regarding quantitative equivalency of dose–response relationships in experimental animals and in humans, a topic that is much debated, controversial, and yet of major consequence for the estimation of human risk (*26–28*). This applies a fortiori when analyses employ estimates of internal doses provided by pharmacokinetic modeling; far from obviating assumptions about toxicological equivalence across species, the use of pharmacokinetics moves the issue of toxicological equivalency to the unfamiliar ground of internal dosimetry.

The second step is partly a matter of convenience, rendering potencies measured in unusual or difficult-to-calculate units (such as those of pharmacokinetically defined target-organ doses) into units more readily compared with measured human exposures. Nevertheless, the reexpression of units can involve key assumptions that should be noted explicitly. For instance, this step may involve using human pharmacokinetic models to "back calculate" from internal doses (on which the dose–response analysis may have been based) to the human exposure scenarios that would lead to them. Such calculations hinge on uncertainties in the human pharmacokinetic model and may involve consequential assumptions about dose-rate effects and route-to-route equivalency. Importantly, it is typically assumed that human pharmacokinetics are essentially linear (i.e., that external exposures as measured are proportional to internal dose) over the range of human exposure levels of interest. This assumption may fail for certain episodic exposures to high levels or when the internal dose measure refers to peak concentrations. For low environmental exposures, however, tissue levels will be far below those leading to saturation of metabolic processes (*6,9*), and all model equations will be essentially linear.

Pharmacokinetic Models and Internal Doses

Target-organ exposures to specific TCE metabolites are hypothesized to be appropriate internal dosimeters (*16,17,19*); therefore, pharmacokinetic models useful to the risk assessment process must describe the metabolic generation and disposition of these moieties in experimental rats and mice and in humans. At present, two models have such capability, one formulated by Fisher (*9*) and one by Clewell et al. (*6*). The models are similar, representing separate elaborations and extensions of a model published by Allen and Fisher (*5*) and Fisher and Allen (*8*). They nonetheless predict some different pharmacokinetic behavior, chiefly in the exposure levels leading to saturation of oxidative metabolism, in the internal doses achieved by inhalation versus gavage in mice, and in the levels of key metabolites to be expected.

Evaluation and comparison of the performance of these models are beyond the scope of the present article, but it is of interest to examine their consequences for the quantitative analysis of the carcinogenicity of TCE. Accordingly, estimates of internal dosimeters calculated from these models by their authors were employed as described below, and references herein to Fisher or Clewell doses refer to these calculations. Development of these models is an ongoing process, and the estimates used here should be regarded as provisional.

Bois (*29,30*) has subjected both the Fisher and Clewell models to a process of uncertainty analysis that includes Bayesian updating of uncertainty distributions of the parameters of the models in view of the performances of the models in explaining various pharmacokinetic data sets. As described in these reports, this results in output distributions of the modeled estimates of internal doses resulting from specified exposure regimes; the distributions represent uncertainty about the value of the internal dose estimates that results from uncertainty about the values of the input parameters. I have used the medians of these

output distributions as an alternative source of central estimates of the internal dosimeters; these values may be regarded as resulting from a Bayesian refining of the values of parameters in the models while retaining the mathematical model structure. I shall refer to these estimates as the Bois-F and Bois-C estimates to indicate the calculations of Bois based on the Fisher and Clewell models, respectively.

Cross-Species Equivalency of Doses

As noted, the definition of relative doses in experimental animals and humans that are expected to yield equal lifetime cancer risks is a matter of ongoing discussion and debate. In this document, I investigate some alternative approaches, but the "base case" is founded on default assumptions mentioned in the new guidelines proposal:

- For oral exposures, the default is to presume that equal toxicity is achieved when daily administered amounts (in milligrams) are equal per unit of body mass to the 3/4 power (*10,26*).
- For inhalation exposures, the default is to follow the dosimetry methodology developed for reference concentrations (*10,31*), which varies with the nature of the compound.

For TCE, the inhalation method used is that for a partly water-soluble gas limited in uptake by lung perfusion (i.e., a category 3 gas) that has chronic systemic toxic effects (*31*). Because the animal:human ratio of blood:air partition coefficients exceeds unity (*6*), the daily concentration × time product, when suffered for a full lifetime, is presumed to yield equal carcinogenic effects in experimental animals and humans.

The scaling of administered doses discussed above is intended to define exposures that are toxicologically equivalent (i.e., producing equal lifetime cancer risks) in experimental rodents and in humans. As such, the scaling method must presume to address systematic species differences in pharmacokinetics (affecting the relative levels of target-organ exposure that result from each daily dose) as well as species differences in pharmacodynamics (affecting the degree of lifetime cancer risk engendered by ongoing daily exposure of the target organ).

Compound-specific pharmacokinetic models address the first of these components, replacing general default principles with compound- and species-specific analysis, but they do not address the second pharmacodynamic aspect. How to express target-organ exposures that emerge from pharmacokinetic analysis so as to be presumed of equivalent lifetime cancer risk in experimental rodents and humans has proved to be a complex and controversial question (*26–28,32–34*). The approach taken herein is to presume that exposures leading to equal daily increments of the area under the concentration–time curve (AUC) of the relevant toxic metabolite in its target organ, when experienced for a full lifetime, will lead to equal elevation of lifetime cancer risk. This is a common assumption for assessment of chronic toxicity corresponding to the notion that equal long-term average tissue concentrations are toxicologically equivalent when experienced for equal fractions of a lifetime. It should be recognized, however, that other reasonable assumptions, with notably different consequences, are possible.

Reactive intermediates in the pathways of biological transformation are formed and lost quickly, and such ephemeral metabolic products do not have well-defined areas-under-the-curve. In the present case, a reactive thiol formed during glutathione-dependent metabolism of TCE is thought to be involved in the genesis of rat kidney tumors (*19*), and kidney exposures to this compound are reported by Clewell et al. (*6*) and Bois (*30*) as daily amounts formed per liter of kidney volume. (The Fisher model does not describe conjugative metabolism of TCE.) Two alternatives for toxic equivalency of this dose measure are entertained: to assume equal carcinogenic effect from equal lifetime average daily production, and to assume equal effect when daily production is proportional to the 3/4-power of body mass. The latter approach is based on the idea that the relatively slower pace of physiological processes in larger species [which tend to maintain proportionality to the 3/4-power of body mass (*35,36*)] is key to scaling the pharmacodynamic processes as well as the pharmacokinetic processes across species. This approach assigns equal chronic toxicity not to the amount of reactive compound produced per unit of tissue over the span of a day but to the same production over equal spans of physiological time. (Since relative areas-under-the-curve already incorporate the slower physiological pace of humans vis-à-vis rodents, a similar allowance for physiological time is not needed when AUCs are the internal dose measure, under this view.)

Mouse Liver Tumors

The toxicology, tumorigenicity, and potential mechanisms of carcinogenic action of TCE in the liver are reviewed by Bull (*16*). TCE has been shown to cause hepatocellular adenomas and carcinomas in both sexes of $B6C3F_1$ mice when administered by corn oil gavage or by inhalation. Some bioassays of other strains of mice have shown liver tumors [e.g., Swiss mice (*22*)], whereas others have shown no such increase [e.g., ICR mice (*37*)]. Bioassays of hamsters (*21*) and several strains of rats (*3,4*) have not shown evidence of liver tumorigenicity by TCE. Epidemiologic studies have produced what the International Agency for Research on Cancer characterizes as "limited" evidence of liver carcinogenicity in exposed humans, based on studies of limited power and consistency (*38*).

It is noteworthy that three of the principal metabolites of TCE—TCA, DCA, and chloral (CH)—are stable compounds that have been shown to cause mouse liver tumors in their own right when administered in drinking water or (in the case of CH) by gastric intubation (*11–15*) [reviewed by Bull (*16*)]. These are three metabolites of the oxidative pathway of TCE metabolism (as opposed to the conjugative pathway hypothesized to be responsible for the rat kidney tumors). The question is raised whether metabolic generation of these compounds in animals dosed with TCE is sufficient to explain the observed induction of liver tumors in these animals. It is also of interest to seek evidence regarding whether the effects of TCE can be ascribed mainly to one or another metabolite, forming the basis for internal-dose analyses and extrapolation to humans. At present, no pharmacokinetic model allows estimation of internal doses of metabolically generated chloral.

Neither TCE nor TCA appears to be genotoxic, and the evidence on CH is debated, as there is some evidence that it can act as a clastogen (*16,39*). In an article in this monograph, DCA is characterized as genotoxic only at high dose levels well above those expected at environmental exposure levels (*39*). Several hypotheses regarding the mechanism of carcinogenic action of TCE suggest underlying processes that might be markedly nonlinear. It is therefore of particular interest to examine the shapes of observed dose–response relationships, seeking evidence of such nonlinear behavior and information regarding the dose ranges in which they may appear.

The data for the mouse bioassays showing liver tumors are presented in Table 1. Administered doses (lifetime average daily doses in mg/kg/day intake) and internal doses based on the pharmacokinetic modeling of Fisher (*9*), Clewell et al. (*6*), and Bois (*29,30*) are also shown. These bioassays have been reviewed and their suitability for risk assessment commented on in more detail by Bull (*16*) and the U.S. EPA (*1,2*). It should be noted that the National Cancer Institute (NCI) (*40*) experiment employed industrial-grade TCE that was contaminated with a stabilizer, epichlorohydrin, that is a cause of site-of-contact tumors. All bioassays used $B6C3F_1$ mice, except for two Maltoni et al. (*22*) experiments on Swiss mice. Maltoni et al. followed their mice until death, so a lifetime of 104 weeks has been assumed. Of the pharmacokinetic doses, only those of Fisher are based on distinct model parameterizations

for males and females, and it should be realized that the Fisher (and Bois-F) doses represent integrated liver concentrations, whereas the Clewell (and Bois-C) doses represent integrated plasma concentrations (which are presumed proportional to the uncharacterized liver concentrations).

Plots of Liver Tumor Response against Various Hypothesized Dose Measures

Several interesting questions may be addressed by plotting liver tumor risk as a function of the alternative dose measures for these data sets:

- whether these various data sets on mouse liver tumors are in general agreement;
- how the potency of TCE in generating mouse liver tumors depends on whether it is administered by corn oil gavage or by inhalation;
- the general dose–response shapes shown by the various experiments, especially evidence for nonlinearity within the observed range;
- whether any such nonlinearity is ascribable to nonlinear pharmacokinetics or to nonlinearity of response vis-à-vis target-organ dose; and
- how different hypothesized dose measures change the dose–response shapes and affect the congruity among the different data sets.

Such plots can serve as evidence regarding which internal dosimeter may be appropriate—presumably, a good target-organ dosimeter will succeed at reconciling responses in experiments of different route and dose levels, portraying them as manifestations of a single underlying relationship of target-organ dose to response (*41,42*).

Plots of the tumor incidence data from Table 1 (not shown) are hampered in visual interpretation by the markedly different

Table 1. Mouse liver tumor incidences and doses.[a]

Bioassay	Sex/strain	LADD (mg/kg/day)	Malignant	Benign + malignant	TCA–auc doses				DCA–auc doses			
					Fisher	Bois-F	Clewell	Bois-C	Fisher	Bois-F	Clewell	Bois-C
NCI (*40*)												
Gavage (mg/kg/day)												
0	Males	0	1/20									
1,000–1,200		724	26/50		1,339	5,715	1,069	1,115	16.5	58.4	14.0	36.5
2,000–2,400		1,448	31/48		2,394	6,032	1,270	1,400	29.5	61.6	17.0	44.0
0	Females	0	0/20									
700–900		538	4/50		924	5,555	986	990	11.4	56.9	12.6	33.0
1,400–1,800		1,076	11/47		1,603	5,896	1,184	1,300	19.7	60.3	15.6	41.0
NTP (*4*)												
Gavage (mg/kg/day)												
0	Males	0	8/48	14/48								
1,000		714	31/50	39/50	1,354	6,504	1,184	1,100	16.7	66.5	15.3	36.0
0	Females	0	2/48	6/48								
1,000		714	13/49	22/49	1,196	6,504	1,184	1,100	14.7	66.5	15.3	36.0
Bell et al. (*43*)												
Inhalation (ppm)												
0	Males	0	18/99	20/99								
100		169	28/95	35/95	257	214	798		0.9	2.2	6.7	
300		508	31/100	38/100	755	608	1,322		2.7	6.2	17.3	
600		1,016	43/97	53/97	1,349	1,059	1,748		4.7	10.8	24.0	
0	Females	0	6/99	8/99								
100		169	4/100	9/100	251	214	798		0.9	0.9	6.7	
300		508	9/94	10/94	708	608	1,322		2.5	2.5	17.3	
600		1,016	13/99	17/99	1,093	1,059	1,748		3.8	3.8	24.0	
Maltoni et al. (*22*)												
Inhalation (ppm)												
0	Males	0	1/85									
100	(BT306)	148	1/86		225	186	687	500	0.8	1.9	5.8	19.0
300		445	3/88		661	530	1,135	970	2.3	5.4	15.1	32.0
600		889	6/88		1,174	918	1,488	1,300	4.1	9.4	20.8	40.0
0	Females	0	3/90									
100		148	4/90		220	186	687	500	0.8	1.9	5.8	19.0
300		445	4/89		618	530	1,135	970	2.2	5.4	15.1	32.0
600		889	9/87		943	918	1,488	1,300	3.3	9.4	20.8	40.0
0	Males	0	17/90									
100	(BT306bis)	148	19/89		225	186	687	500	0.8	1.9	5.8	19.0
300		445	27/90		661	530	1,135	970	2.3	5.4	15.1	32.0
600		889	21/90		1,174	918	1,488	1,300	4.1	9.4	20.8	40.0
0	Males	0	4/88									
100	(Swiss)	148	2/89		225	186	687	500	0.8	1.9	5.8	19.0
300		445	8/89		661	530	1,135	970	2.3	5.4	15.1	32.0
600		889	13/90		1,174	918	1,488	1,300	4.1	9.4	20.8	40.0
0	Females	0	0/90									
100	(Swiss)	148	0/89		220	186	687	500	0.8	1.9	5.8	19.0
300		445	0/89		618	530	1,135	970	2.2	5.4	15.1	32.0
600		889	1/89		943	918	1,488	1,300	3.3	9.4	20.8	40.0

LADD, lifetime average daily dose (intake), allowing for dose-rate changes in NCI (*40*) and nondosed days during and at end of experiment. [a]Tumor incidences corrected for early mortality by removing from consideration animals that died before first appearance of tumor of interest. For Maltoni et al. (*22*) malignant tumors are hepatomas; for all others, benign and malignant tumors are hepatocellular adenomas and carcinomas, respectively. Fisher (*9*) and Bois-F (*30*) doses are daily integrated liver concentrations. Clewell et al. (*6*) and Bois-C (*29*) doses are daily integrated plasma concentrations, all in (mg-hr)/L.

background rate among data sets. It is not altogether clear why controls differ so much in liver tumor incidence among studies. More informative plots (Figure 1) are obtained if the incidence rate in controls is subtracted from that of each dosed group in an experiment.

When plotted against administered dose (or, for inhalation, daily intake) in mg/kg/day, the male mice show general agreement among the gavage studies on the one hand and among the inhalation studies on the other (Figure 1a). But in these dose units, TCE from inhalation appears systematically less potent than from corn oil gavage. Among inhalation studies, the response appears to increase gradually with intake, whereas the gavage doses seem to show a plateau of response, with no dose point at a dose low enough to provide evidence for or against nonlinearity at lower doses. Female mice (plots not shown) show lower incidences than males and evince less differentiation between inhalation and gavage studies.

When responses are plotted against the Fisher estimates of the area under the concentration–time curve for TCA (TCA–auc) (Figure 1b), the pattern appears very similar, a consequence of the high degree of proportionality of the Fisher TCA–auc estimates and intake. On this plot, employing TCA–auc dosimetry fails to reconcile inhalation and gavage experimental outcomes in terms of a single relationship of internal dose to response.

When responses are plotted against the TCA–auc emerging from the Bois reanalysis of the Fisher model (Figure 1c), two major changes are evident. Inhalation exposures are modeled as producing much smaller TCA–auc than gavage doses (due mostly to an increase in the estimates from gavage doses). This leads to the possible interpretation that the inhalation and gavage responses might be drawn from the lower and higher regions of a single internal dose versus response relationship. Second, a high degree of saturation of TCA production is evident between the low and high gavage doses; despite an administered amount that is twice as great, the high NCI gavage dose has a modeled TCA–auc that is only slightly above that of the lower dose. Indeed, the similar tumor responses at the single NTP bioassay dose level and at the two dose levels in the NCI study are explicable in terms of their similar TCA–auc (Table 1).

TCA–auc estimates from the Clewell model (Figure 1d) preserve the saturation of TCA production from low to high gavage dose, but inhalation exposures are modeled as producing as high or higher TCA–auc than the gavage dosing. This leads to clear incompatibility of the inhalation and gavage curves based on this dosimeter. The Bois reanalysis of the Clewell model (*29*) (plots not shown) substantially agrees with the original Clewell results.

The liver tumor bioassay results can also be evaluated as potential functions of the other major oxidative metabolite of TCE, dichloroacetic acid. The absolute amounts of DCA, and the areas-under-the-curve they produce, are much smaller than for TCA, but reasons to consider DCA as the potentially responsible metabolite exist (*16*). Using the Fisher model estimates of DCA area under the concentration–time curve (DCA–auc, Figure 1e) shows the same lack of saturation of DCA production between the low and high gavage doses that is seen with TCA. Inhalation exposures are estimated to generate much less DCA than gavage doses, leading to potential interpretation of responses across routes of administration as common reflections of a single underlying relationship with DCA–auc. Doses from the Bois reanalysis of the Fisher model (Figure 1f) lead chiefly to a difference in the high-dose behavior, which (as with his analysis of TCA) shows substantial saturation of DCA production.

The Clewell model estimates of DCA–auc (Figure 1g) are absolutely lower for gavage (but nonetheless showing pronounced saturation) and higher for inhalation exposures. As a result, using this analysis, DCA production fails to reconcile inhalation and gavage responses.

For the Clewell model (and for the Bois reanalysis), calculations were also made of peak concentrations of TCA and DCA, with the aim of assessing whether the higher concentrations achieved by bolus dosing might have demonstrable toxicological significance. In practice, however, for the exposure regimes of interest, peak concentrations are very highly correlated with areas under the curve, and the plots of response as a function of peak concentration (not shown) hardly differ from those against TCA–auc and DCA–auc. Plots of responses in female mice are not shown, but they give results generally similar to those for males, although the incompatibility of gavage and inhalation responses is not as marked.

In sum, the most notable feature of the plotting exercise is the high degree of dependence on which pharmacokinetic model is employed to generate estimates of internal doses. The computed estimates are not only numerically different, they also show different patterns of dose dependence of metabolic generation of TCA and DCA and different degrees of difference between gavage and inhalation exposures.

The two gavage experiments produced outcomes that are mutually compatible, and the suite of inhalation bioassays are also largely mutually consistent in outcome, but the ability to explain the gavage and inhalation results simultaneously as common reflections of a single underlying dose–response relationship with a measure of target-organ dose is not clear—some dose measures show clear failure of reconciliation, and others are at best ambiguous. Unfortunately, the plots appear to provide little evidence regarding whether TCA or DCA (expressed either as AUCs or as peak concentrations) are primarily responsible for the mouse liver tumors.

The pharmacokinetic dose measures (except those from the Fisher model) show similar internal doses at the low and high gavage levels, explaining the similarity in tumor response. In essence, there is a single high internal dose that has been tested 3 times with similar outcome, but these data give little information about the shape of the dose–response relationship. In contrast, the inhalation studies have a series of lower doses of increasing magnitude, and these studies evince a more-or-less gradually increasing response with internal dose that shows no signs of pronounced nonlinearity in the observable range.

Dose–Response Analysis

Dose–response curves were fitted to the data sets in Table 1 using administered dose (mg/kg/day intake), ppm-hours of exposure (for the inhalation studies), and the various proposed internal dose metrics based on the pharmacokinetic modeling of Fisher (*9*), Clewell et al. (*6*), and Bois (*29,30*). In essence, basing an analysis on estimates of TCA–auc or DCA–auc represents an examination of the consequences of ascribing the observed tumorigenicity of TCE entirely to the actions of the one or of the other metabolite.

For nearly all the inhalation studies using any dose metric, the maximum likelihood curve is linear [the exceptions being the Bell et al. females (*43*) and the Maltoni et al. Swiss males (*22*)]. Moreover, the ED_{10} values obtained are generally larger (i.e., the potencies are lower) than those seen for the corn oil gavage data sets, to a degree that varies with the dose metric used. For this reason, the inhalation analyses are not shown, and the following focuses on the results from the gavage studies.

The estimated ED_{10} and LED_{10} values obtained for the gavage studies are shown in Table 2. Since the NTP study (*4*) had but one positive dose level, the estimated curves are, of mathematical necessity, linear in dose, although a substantial power of time is estimated in the time-to-tumor analyses. For the NCI data (*40*), owing to the points being nearly superimposed (Figure 1), there is little opportunity to illuminate the dose–response pattern. In an attempt to gain perspective on the curve shape in the observable range, analyses were conducted on the pooled data of the NCI and NTP studies (results not shown), but the similarity in response and (for most dose measures) internal dose for all three dosed groups prevents results from differing substantially from the analyses of single studies.

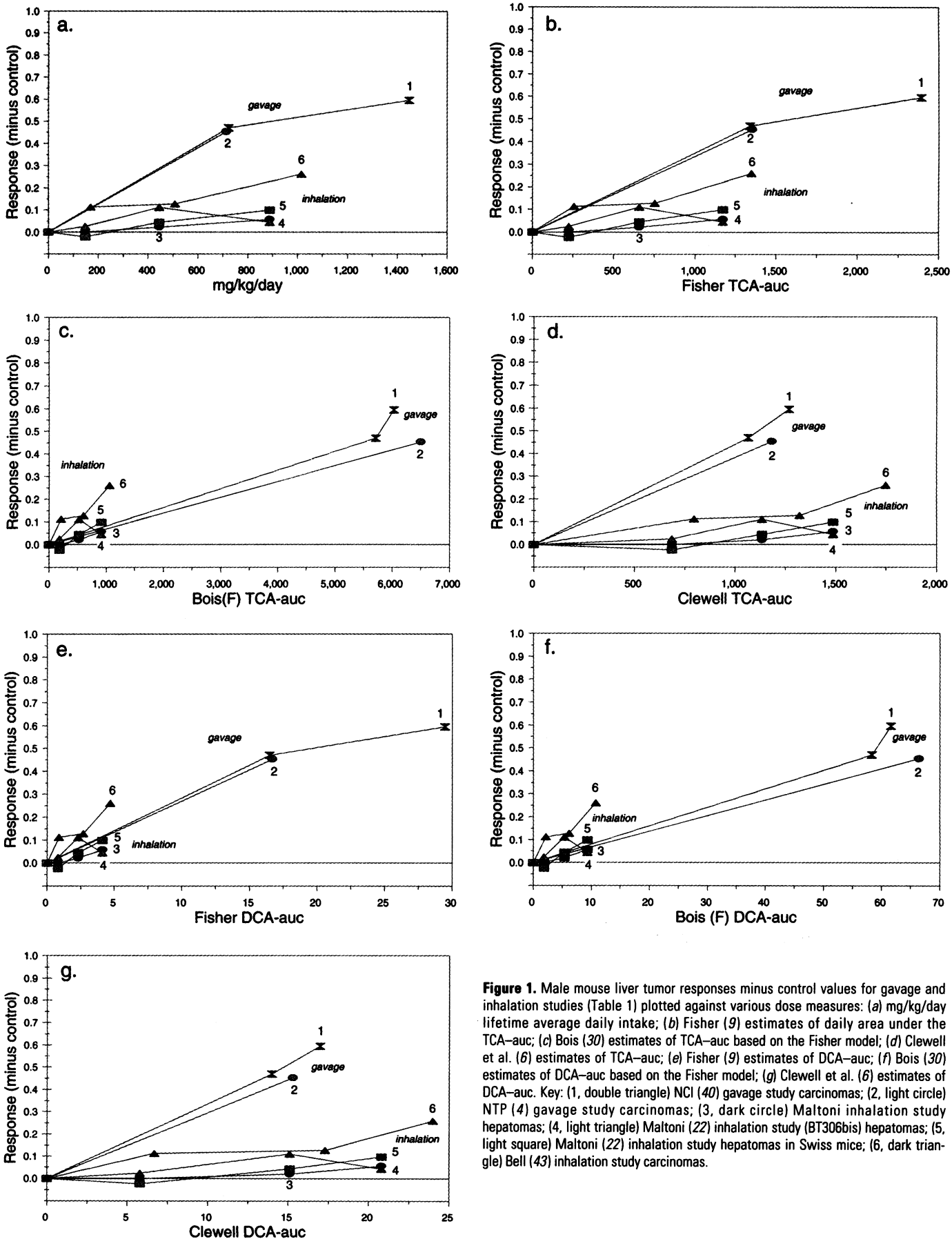

Figure 1. Male mouse liver tumor responses minus control values for gavage and inhalation studies (Table 1) plotted against various dose measures: (*a*) mg/kg/day lifetime average daily intake; (*b*) Fisher (*9*) estimates of daily area under the TCA–auc; (*c*) Bois (*30*) estimates of TCA–auc based on the Fisher model; (*d*) Clewell et al. (*6*) estimates of TCA–auc; (*e*) Fisher (*9*) estimates of DCA–auc; (*f*) Bois (*30*) estimates of DCA–auc based on the Fisher model; (*g*) Clewell et al. (*6*) estimates of DCA–auc. Key: (1, double triangle) NCI (*40*) gavage study carcinomas; (2, light circle) NTP (*4*) gavage study carcinomas; (3, dark circle) Maltoni inhalation study hepatomas; (4, light triangle) Maltoni (*22*) inhalation study (BT306bis) hepatomas; (5, light square) Maltoni (*22*) inhalation study hepatomas in Swiss mice; (6, dark triangle) Bell (*43*) inhalation study carcinomas.

The ED_{10} and LED_{10} values of Table 2 can be used as Points of Departure. In the case of TCA–auc and DCA–auc, it is assumed that humans will have the same lifetime cancer risk when exposed to similar daily increments of area under the concentration curve of these metabolites (that is, they apply as is without further adjustment), whereas the projection of the administered dose values to humans assumes equal risk for mg/kg$^{3/4}$/day exposure. Low-dose slopes for the U.S. EPA proposed linear method can be obtained by dividing 0.1 by the appropriate ED_{10} or LED_{10} (*10*).

For each source of internal dosimetry estimates, Table 3 shows the internal dose in humans that would result from ongoing exposure to one conventional unit of external environmental concentration. These human internal doses can then be multiplied by the corresponding linear-method slope (which is in terms of risk per unit of internal exposure), to generate the incremental human risk per unit of conventional exposure, that is, a unit risk of the conventional sort except that it is derived based on dose–response analysis and cross-species extrapolation using the internal dosimetry, as described by the relevant pharmacokinetic model. (This method assumes that, at relevant human exposure levels, human internal doses are proportional to external exposures, which is true in the present case.)

Table 4 presents human incremental risks per unit of mg/kg/day intake calculated in this way. Each tabulated value is an alternative estimate based on the data set of the row and using the dose metric of the column for dose–response analysis and animal-to-human extrapolation. Table 5 gives incremental risk per µg/L of drinking water contamination, on the assumption of lifetime consumption of 2 L/day. Table 6 shows incremental risk per µg/m^3 of ambient air concentration on the assumption of continuous lifetime exposure. It should be clear that the last table represents a route extrapolation of the gavage study in mice to human inhalation, using a human inhalation pharmacokinetic model (including its breathing rate) to estimate the human liver dose of TCA or DCA, on the assumption that a given area under the curve in human liver will have the same risk whether it derives from an original oral or inhalation exposure.

Points of Departure, expressed as the human externally measured exposures necessary to engender a 10% extra risk level [which are used in defining the Margin of Exposure of the U.S. EPA nonlinear method (*10*)] can be obtained by multiplying the reciprocals of the entries of Tables 4–6 by 0.1.

Analysis of TCA and DCA Bioassays

Both TCA and DCA, the principal stable metabolites of oxidative metabolism of TCE, have been shown to be carcinogenic in their own right when administered in drinking water (*11–16*). For neither compound has a full lifetime bioassay of the usual design been conducted, but a number of studies have examined mice for various durations of exposure to a variety of drinking water concentrations (Table 7). It is largely due to these observations that DCA and TCA are candidates for the ultimate cause of the liver carcinogenicity of TCE. It is therefore of interest to examine the carcinogenic potency of DCA and TCA as a means of asking whether the tumors engendered by TCE can be quantitatively explained on the basis of the DCA and TCA (measured as their areas under the curve metabolically generated as a consequence of TCE dosing. In addition, evidence of nonlinear tumor response curves as a function of either DCA or TCA exposure could provide insight into the low-dose shape

Table 2. LED_{10} and ED_{10} values based on mouse liver tumors.

Data set	Administered, mg/kg/day	TCA–auc, (mg-hr)/L				DCA–auc, (mg-hr)/L		
		Fisher	Bois-F	Clewell	Bois-C	Fisher	Clewell	Bois-C
ED_{10}								
NTP (*4*)								
Males, carcinomas	60.4	114.6	550.6	100.2	93.1	1.41	1.3	3.05
Males, adenomas + carcinomas	35.2	66.8	320.9	58.4	54.3	0.82	0.75	1.78
Females, carcinomas	167.9	281.2	1,529.5	278.4	258.7	3.46	3.6	8.47
Females, adenomas + carcinomas	73.5	123.1	669.5	121.9	113.2	1.51	1.57	3.71
NCI (*40*)								
Males, carcinomas	136.8	234.8	4,168.5	417.2	302.4	2.89	5.02	13.99
Females, carcinomas	621.8	1,039.9	5,297.0	856.9	905.8	12.82	11.14	29.23
LED_{10}								
NTP (*4*)								
Males, carcinomas	37.8	71.7	344.2	62.7	58.2	0.88	0.81	1.91
Males, adenomas + carcinomas	21.6	40.9	196.5	35.8	33.2	0.5	0.46	1.09
Females, carcinomas	90.7	151.9	825.9	150.4	139.7	1.87	1.94	4.57
Females, adenomas + carcinomas	43.9	73.5	399.8	72.8	67.6	0.9	0.94	2.21
NCI (*40*)								
Males, carcinomas	106.5	183.5	624.8	119.4	126.7	2.26	1.57	4.09
Females, carcinomas	348.9	573.6	2,885.6	495.7	535.2	7.07	6.5	17.08

NTP analyses are based on Multistage-Weibull time-to-tumor analysis; NCI analyses are based on multistage model of degree 2. Fisher (*9*) and Bois-F (*30*) doses are AUC in liver; Clewell (*6*) and Bois-C (*29*) doses are AUC in plasma. Bois did not analyze DCA–auc for the Fisher model.

Table 3. Modeled human internal doses from unit environmental exposures.

Model	Human exposure	TCA–auc daily, (mg-hr)/L		DCA–auc daily, (mg-hr)/L		Thiol production daily, mg/g-kidney	Chloral–auc daily, (mg-hr)/L
		In liver	In plasma	In liver	In plasma		
Fisher (*9*)	1 ppb inhalation	0.1253		3.77×10^{-4}			
	1 µg/L in drinking water ($= 2.86 \times 10^{-5}$ mg/kg/day)	0.0062		1.87×10^{-5}			
Bois (*30*) (Bois-F)	1 µg/L in drinking water	0.0038					
Clewell et al. (*6*)	1 ppm inhalation		303		0.025	0.008	0.002
	1 mg/L in drinking water		14		0.0011	0.0004	2×10^{-5}
Bois (*29*) (Bois-C)	1 ppm inhalation		88		0.45	0.11	0.0013
	1 mg/L in drinking water		4.2		0.027	0.0060	2.3×10^{-6}

Table 4. Linear method estimates of incremental risk per mg/kg/day of TCE intake based on mouse liver tumors.

Data set	Dose metric: mg/kg$^{3/4}$/day intake	TCA–auc, (mg-hr)/L: Fisher	TCA–auc, (mg-hr)/L: Bois-F	TCA–auc, (mg-hr)/L: Clewell	TCA–auc, (mg-hr)/L: Bois-C	DCA–auc, (mg-hr)/L: Fisher	DCA–auc, (mg-hr)/L: Clewell	DCA–auc, (mg-hr)/L: Bois-C
Based on ED_{10} values								
NTP (*4*)								
Males, carcinomas	1.1×10^{-2}	1.9×10^{-1}	2.4×10^{-2}	4.9×10^{-1}	1.6×10^{-1}	4.6×10^{-2}	3.0×10^{-3}	3.1×10^{-2}
Males, adenomas + carcinomas	1.9×10^{-2}	3.3×10^{-1}	4.1×10^{-2}	8.4×10^{-1}	2.7×10^{-1}	7.9×10^{-2}	5.1×10^{-3}	5.3×10^{-2}
Females, carcinomas	4.0×10^{-3}	7.7×10^{-2}	8.7×10^{-3}	1.8×10^{-1}	1.2×10^{-1}	1.9×10^{-2}	1.1×10^{-3}	1.1×10^{-2}
Females, adenomas + carcinomas	9.1×10^{-3}	1.8×10^{-1}	2.0×10^{-2}	4.0×10^{-1}	1.3×10^{-1}	4.3×10^{-2}	2.4×10^{-3}	2.6×10^{-2}
NCI (*40*)								
Males, carcinomas	4.9×10^{-3}	9.2×10^{-2}	6.3×10^{-3}	1.2×10^{-1}	4.9×10^{-2}	2.3×10^{-2}	7.7×10^{-4}	6.8×10^{-3}
Females, carcinomas	1.1×10^{-3}	2.1×10^{-2}	2.9×10^{-3}	5.7×10^{-2}	1.6×10^{-2}	5.2×10^{-3}	3.5×10^{-4}	3.2×10^{-3}
Based on LED_{10} values								
NTP (*4*)								
Males, carcinomas	1.8×10^{-2}	3.3×10^{-1}	3.9×10^{-2}	7.8×10^{-1}	2.5×10^{-1}	7.4×10^{-2}	4.8×10^{-3}	5.0×10^{-2}
Males, adenomas + carcinomas	3.1×10^{-2}	5.3×10^{-1}	6.8×10^{-2}	1.3×10^{0}	4.4×10^{-1}	1.3×10^{-1}	8.3×10^{-3}	8.7×10^{-2}
Females, carcinomas	7.4×10^{-3}	1.4×10^{-1}	1.6×10^{-2}	3.3×10^{-1}	1.1×10^{-1}	3.5×10^{-2}	2.0×10^{-3}	2.1×10^{-2}
Females, adenomas + carcinomas	1.5×10^{-2}	3.0×10^{-1}	3.3×10^{-2}	6.7×10^{-1}	2.2×10^{-1}	7.2×10^{-2}	4.1×10^{-3}	4.3×10^{-2}
NCI (*40*)								
Males, carcinomas	6.3×10^{-3}	1.2×10^{-1}	2.1×10^{-2}	4.1×10^{-1}	1.2×10^{-1}	2.9×10^{-2}	2.5×10^{-3}	2.3×10^{-2}
Females, carcinomas	1.9×10^{-3}	3.8×10^{-2}	5.4×10^{-3}	9.9×10^{-2}	2.8×10^{-2}	9.3×10^{-3}	5.9×10^{-4}	5.5×10^{-3}

NTP analyses are based on Multistage-Weibull time-to-tumor analysis; NCI analyses are based on multistage model of degree 2. Fisher (*9*) and Bois-F (*30*) doses are AUC in liver; Clewell (*6*) and Bois-C (*29*) doses are AUC in plasma. Bois did not analyze DCA–auc for the Fisher model.

Table 5. Linear method estimates of incremental risk per µg/L of TCE in drinking water based on mouse liver tumors.

Data set	Dose metric: mg/kg$^{3/4}$/day intake	TCA–auc, (mg-hr)/L: Fisher	TCA–auc, (mg-hr)/L: Bois-F	TCA–auc, (mg-hr)/L: Clewell	TCA–auc, (mg-hr)/L: Bois-C	DCA–auc, (mg-hr)/L: Fisher	DCA–auc, (mg-hr)/L: Clewell	DCA–auc, (mg-hr)/L: Bois-C
Based on ED_{10} values								
NTP (*4*)								
Males, carcinomas	3.2×10^{-7}	5.4×10^{-6}	6.9×10^{-7}	1.4×10^{-5}	4.5×10^{-6}	1.3×10^{-6}	8.5×10^{-8}	8.9×10^{-7}
Males, adenomas + carcinomas	5.4×10^{-7}	9.3×10^{-6}	1.2×10^{-6}	2.4×10^{-5}	7.7×10^{-6}	2.3×10^{-6}	1.5×10^{-7}	1.5×10^{-6}
Females, carcinomas	1.1×10^{-7}	2.2×10^{-6}	2.5×10^{-7}	5.0×10^{-6}	3.5×10^{-6}	5.4×10^{-7}	3.1×10^{-8}	3.2×10^{-7}
Females, adenomas + carcinomas	2.6×10^{-7}	5.0×10^{-6}	5.7×10^{-7}	1.2×10^{-5}	3.7×10^{-6}	1.2×10^{-6}	7.0×10^{-8}	7.3×10^{-7}
NCI (*40*)								
Males, carcinomas	1.4×10^{-7}	2.6×10^{-6}	1.8×10^{-7}	3.4×10^{-6}	1.4×10^{-6}	6.5×10^{-7}	2.2×10^{-8}	1.9×10^{-7}
Females, carcinomas	3.1×10^{-8}	6.1×10^{-7}	8.4×10^{-8}	1.6×10^{-6}	4.6×10^{-7}	1.5×10^{-7}	9.9×10^{-9}	9.2×10^{-8}
Based on LED_{10} values								
NTP (*4*)								
Males, carcinomas	5.1×10^{-7}	8.7×10^{-6}	1.1×10^{-6}	2.2×10^{-5}	7.2×10^{-6}	2.1×10^{-6}	1.4×10^{-7}	1.4×10^{-6}
Males, adenomas + carcinomas	8.9×10^{-7}	1.5×10^{-5}	1.9×10^{-6}	3.9×10^{-5}	1.3×10^{-5}	3.7×10^{-6}	2.4×10^{-7}	2.5×10^{-6}
Females, carcinomas	2.1×10^{-7}	4.1×10^{-6}	4.6×10^{-7}	9.3×10^{-6}	3.0×10^{-6}	1.0×10^{-6}	5.7×10^{-8}	5.9×10^{-7}
Females, adenomas + carcinomas	4.4×10^{-7}	8.4×10^{-6}	9.5×10^{-7}	1.9×10^{-5}	6.2×10^{-6}	2.1×10^{-6}	1.2×10^{-7}	1.2×10^{-6}
NCI (*40*)								
Males, carcinomas	1.8×10^{-7}	3.4×10^{-6}	6.3×10^{-7}	1.2×10^{-5}	3.3×10^{-6}	8.3×10^{-7}	7.0×10^{-8}	6.6×10^{-7}
Females, carcinomas	5.5×10^{-8}	1.1×10^{-6}	1.5×10^{-7}	2.8×10^{-6}	7.9×10^{-7}	2.7×10^{-7}	1.7×10^{-8}	1.6×10^{-7}

Based on lifetime consumption of contaminated water at 2 L/day. NTP analyses are based on Multistage-Weibull time-to-tumor analysis; NCI analyses are based on multistage model of degree 2. Fisher (*9*) and Bois-F (*30*) doses are AUC in liver; Clewell (*6*) and Bois-C (*29*) doses are AUC in plasma. Bois did not analyze DCA–auc for the Fisher model.

expected for TCE (which is not very well illuminated by analysis of TCE dose–response relationships, as discussed above).

Because of the unusual experimental designs, no single study on either DCA or TCA is suitable for the determination of a lifetime cancer potency, but one can gain some insight through pooling the results from several studies, treating the differing duration of the tests as different times of "interim" scheduled sacrifice in a Multistage-Weibull time-to-tumor analysis. TCA–auc and DCA–auc values (Table 7) were obtained from a version of the Fisher pharmacokinetic model modified to accommodate uptake of these compounds from drinking water (*9,30*). In the case of DCA, a single dose-time–response relationship could describe all the liver tumor results among male mice, but the inclusion of the single female data set (*15*) led to a poor fit. For TCA, a single equation fit all of the responses well, but females were excluded (with little change in estimated potency) for consistency with the DCA analysis and for comparison with the male mouse TCE gavage studies.

Figure 2 shows the resulting dose–response curves for the expected frequency of liver carcinomas after 90 and 104 weeks (the durations of the NCI and NTP studies, respectively) as a function of increasing internal dose. Also plotted are the actual TCE gavage responses among NCI and NTP males, plotted as a function of their metabolically generated internal doses. For the Fisher estimates of TCA–auc (Figure 2a), these responses are much higher than would be expected if they were solely due to metabolically generated TCA, judging from the apparent potency of TCA when administered directly. According to the TCA bioassay curves, responses of about 60% would be expected at daily TCA–auc levels of around 6,000 (mg-hr)/L, some 3- to 4-fold higher than the estimated exposure to metabolically generated TCA in the TCE gavage studies. In contrast, the Bois-F estimates (Figure 2b) show the TCE gavage results to be very close to what would be expected if they were due solely to metabolically generated TCA.

For DCA, the dose estimates from the Fisher model (Figure 2c) show metabolically

Table 6. Linear method estimates of incremental risk per per μg/m^3 of TCE in ambient air based on mouse liver tumors.

Data set	Dose metric: mg/kg$^{3/4}$/day intake	TCA–auc, (mg-hr)/L: Fisher	TCA–auc, (mg-hr)/L: Bois-F	TCA–auc, (mg-hr)/L: Clewell	TCA–auc, (mg-hr)/L: Bois-C	DCA–auc, (mg-hr)/L: Fisher	DCA–auc, (mg-hr)/L: Clewell	DCA–auc, (mg-hr)/L: Bois-C
Based on ED_{10} values								
NTP (*4*)								
Males, carcinomas	3.2×10^{-6}	2.1×10^{-5}	2.6×10^{-6}	5.6×10^{-5}	1.8×10^{-5}	5.0×10^{-6}	3.6×10^{-7}	2.7×10^{-6}
Males, adenomas + carcinomas	5.4×10^{-6}	3.6×10^{-5}	4.5×10^{-6}	9.6×10^{-5}	3.0×10^{-5}	8.5×10^{-6}	6.2×10^{-7}	4.7×10^{-6}
Females, carcinomas	1.1×10^{-6}	8.5×10^{-6}	9.5×10^{-7}	2.2×10^{-5}	1.3×10^{-5}	2.0×10^{-6}	1.3×10^{-7}	9.9×10^{-7}
Females, adenomas + carcinomas	2.6×10^{-6}	1.9×10^{-5}	2.2×10^{-6}	4.6×10^{-5}	1.4×10^{-5}	4.6×10^{-6}	3.0×10^{-7}	2.3×10^{-6}
NCI (*40*)								
Males, carcinomas	1.4×10^{-6}	1.0×10^{-5}	6.9×10^{-7}	1.4×10^{-5}	5.4×10^{-6}	2.4×10^{-6}	9.3×10^{-8}	6.0×10^{-7}
Females, carcinomas	3.1×10^{-7}	2.3×10^{-6}	3.2×10^{-7}	6.6×10^{-6}	1.8×10^{-6}	5.6×10^{-7}	4.2×10^{-8}	2.9×10^{-7}
Based on LED_{10} values								
NTP (*4*)								
Males, carcinomas	5.1×10^{-6}	3.3×10^{-5}	4.2×10^{-6}	9.0×10^{-5}	2.8×10^{-5}	7.9×10^{-6}	5.7×10^{-7}	4.4×10^{-6}
Males, adenomas + carcinomas	8.9×10^{-6}	5.8×10^{-5}	7.4×10^{-6}	1.6×10^{-4}	4.9×10^{-5}	1.4×10^{-5}	1.0×10^{-6}	7.7×10^{-6}
Females, carcinomas	2.1×10^{-6}	1.6×10^{-5}	1.8×10^{-6}	3.8×10^{-5}	1.2×10^{-5}	3.8×10^{-6}	2.4×10^{-7}	1.8×10^{-6}
Females, adenomas + carcinomas	4.4×10^{-6}	3.2×10^{-5}	3.6×10^{-6}	7.7×10^{-5}	2.4×10^{-5}	7.8×10^{-6}	4.9×10^{-7}	3.8×10^{-6}
NCI (*40*)								
Males, carcinomas	1.8×10^{-6}	1.3×10^{-5}	2.4×10^{-6}	4.7×10^{-5}	1.3×10^{-5}	3.1×10^{-6}	3.0×10^{-7}	2.0×10^{-6}
Females, carcinomas	5.5×10^{-7}	4.2×10^{-6}	5.8×10^{-7}	1.1×10^{-5}	3.1×10^{-6}	9.9×10^{-7}	7.2×10^{-8}	4.9×10^{-7}

Based on continuous lifetime exposure. Human breathing rates as in the applicable pharmacokinetic model or (for intake) 20 m^3/day. NTP analyses are based on Multistage-Weibull time-to-tumor analysis; NCI analyses are based on multistage model of degree 2. Fisher (*9*) and Bois-F (*30*) doses are AUC in liver; Clewell (*6*) and Bois-C (*29*) doses are AUC in plasma. Bois did not analyze DCA–auc for the Fisher model.

generated DCA to be markedly insufficient to explain the TCE gavage tumors; doses some 10-fold higher are needed to generate comparable responses when DCA is administered directly. Under the Bois internal dose estimates (Figure 2d), however, the amount of metabolically generated DCA in the TCE gavage studies is more than enough to account for the observed tumors; indeed, a third as much would seem to be sufficient, and under this dosimetry it is not clear why the TCE studies did not have nearly 100% response, given the DCA estimated to have been metabolically produced.

As with previous analyses, the outcome depends markedly on which set of pharmacokinetic results one employs. The dose dependence of the fitted time-to-tumor relationships is linear for directly administered TCA (as is the time dependence), whereas that for DCA is linear–quadratic with a substantial linear contribution, although the time dependence is about the third power of time.

Mouse Lung Tumors

Trichloroethylene has been shown to cause increases in lung tumors in mice chronically exposed by inhalation (*22,37*), although increases are not found in all experiments, despite similar exposures. Lung tumors have not been seen to increase in gavage experiments (*4,40*), and no lung tumor effect has been seen in rats (*3,4*). Although lung tumors appear in mice solely by inhalation exposure, lung tumors are not the only tumors found to be elevated in inhalation experiments; hepatocellular carcinomas have been seen in mice exposed to TCE by inhalation (*22,43*), and rats have been found to have increases in

Table 7. TCA and DCA drinking water experiments in mice—mouse liver tumors.

Bioassay	Conc.in water, g/L	Mice with carcinomas		TCA–auc: Fisher	TCA–auc: Bois-F	DCA–auc: Fisher	DCA–auc: Bois-F
TCA in drinking water							
Herren-Freund et al. (*14*)	TCA	61 weeks					
Male mice	0	0/22		0	0	0	0
	5	7/22		5,138	4,406	63.3	45.0
Bull et al. (*11*)	TCA	37 weeks	52 weeks				
Male mice	0		0/35	0	0	0	0
	1		2/11	1,290	1,106	15.9	11.3
	2	3/11	4/24	2,252	1,931	27.7	19.7
Periera (*15*)	TCA	52 weeks	81 weeks				
Female mice	0	0/40	2/90	0	0	0	0
	0.35	0/40	0/53	570		7.0	
	1.2	0/19	5/27	1,544		19.0	
	3.5	5/20	5/18	3,700	3,173	45.6	32.4
DCA in drinking water							
DeAngelo et al. (*13*)	DCA	60 weeks	75 weeks				
Male mice	0	0/9	2/19			0	0
	0.05	2/9	3/21			14.8	1.38
	0.5	1/9	1/18			138.3	14.0
	5.0	25/30				888.8	88.4
Herren-Freund et al. (*14*)	DCA	61 weeks					
Male mice	0	0/22				0	0
	5.0	21/26				888.8	88.4
Daniel et al. (*12*)	DCA	104 weeks					
Male mice	0	2/20				0	0
	0.5	15/24				138.3	14.0
Periera (*15*)	DCA	52 weeks	81 weeks				
Female mice	0	0/40	2/90			0	
	0.28	0/40	0/50			85.1	
	0.93	0/20	1/28			224.2	
	2.8	1/20	5/19			589.0	
Bull et al. (*11*)	DCA	37 weeks	52 weeks				
Male mice	2	0/11	5/24			420.7	38.7

Fisher DCA–auc for DeAngelo et al. (*13*) accounts for reduced water consumption at 5 g/L; this is assumed to apply to the 5 g/L exposure of Herren-Freund et al. (*14*). Bull et al. (*11*) data as reported in Bull (*16*). NTP analyses based on Multistage-Weibull time-to-tumor analysis; NCI analyses based on multistage model of degree 2. Fisher (*9*) and Bois-F (*30*) doses are AUC in liver; Clewell (*6*) and Bois-C (*29*) doses are AUC in plasma. Bois did not analyze DCA–auc for the Fisher model.

kidney tumors following inhalation in some experiments (*22*) but not in others (*37*).

The toxicology of TCE in the lung is discussed by Green (*17*). Attention has focused on the role of cytotoxicity to mouse lung Clara cells, which are highly metabolically active compared to most cell types in the lung. These cells evince a pattern of cytotoxicity following initial exposure, with a subsequent recovery even upon continued exposure. In a regime of inhalation exposure such as is practiced in cancer bioassays, however, a renewed bout of cytotoxic response can be engendered on each Monday following the cessation of exposure over each weekend. It has been proposed that this toxicity, and the regenerative cell replication that it induces may be responsible for the lung tumors in mice and that the particular susceptibility of mice is attributable to the fact that mouse Clara cells generate a good deal of the metabolite CH by oxidative metabolism of TCE, but they are relatively deficient in chloral metabolic clearance (*44*). Chloral has shown clastogenic activity in some tests (*16,39*). It has been shown to cause the same kind of vacuolization response in Clara cells as does TCE (*44*).

It is difficult accurately to model the concentrations of a metabolite such as CH that is itself quickly metabolized to further products, but both Clewell et al. (*6*) and Bois (*29*) have provided estimates of chloral area-under-the-curve (CH–auc) and maximum concentration (CH–max) in lung. These measures are considered internal dosimeters for the dose–response analysis of the mouse lung tumors generated by TCE exposure.

Tumor data from the mouse bioassays showing lung tumor response are presented in Table 8 along with relevant dose measures. The Maltoni experiments are the same ones in which liver tumors were observed, but no information on co-occurrence of liver and lung tumors among mice was presented.

The tumor data are plotted in Figure 3. The elevations in lung tumor risk are seen to be rather small and somewhat inconsistent among experiments. Several data sets fail to show a monotonic trend with increasing dose. (Plots against exposure concentration and CH–auc look very similar, since the various potential dosimeters are more or less proportional.) With such data, it is hard to address the issue of nonlinearity and the possibility of a point within the observable range at which a change in the underlying mode of action may occur. To the extent that there are consistent trends in some data sets, they show a more or less linear pattern. Best fitting multistage models have only a linear term for the Fukuda data sets and for the Maltoni male Swiss mice; the Maltoni B6C3F$_1$ female mice have a linear-quadratic fit, and only the Maltoni Swiss females have a nonlinear best fit. The two Maltoni B6C3F$_1$ male data sets show no increase with dose.

The results of dose–response analysis are shown in Table 9. For administered doses, attention should be focused on the calculations assuming equivalence of lifetime averaged $\mu g/m^3$ (*10*). The human potencies extrapolated from mouse lung tumors are lower than for the other two prominent end points, even when one considers extrapolations based on administered dose. These are lowered further when internal doses are examined, although more so for the Bois doses than for the Clewell doses. This reflects the relatively lower doses in humans versus mice for a given level of exposure (and appears little affected by high-to-low dose nonlinearity in CH internal dose versus exposure concentration).

Unit risks for ingestion and drinking water exposures based on route extrapolation of the lung tumor risks were calculated but are not shown in Table 9, since they are invariably

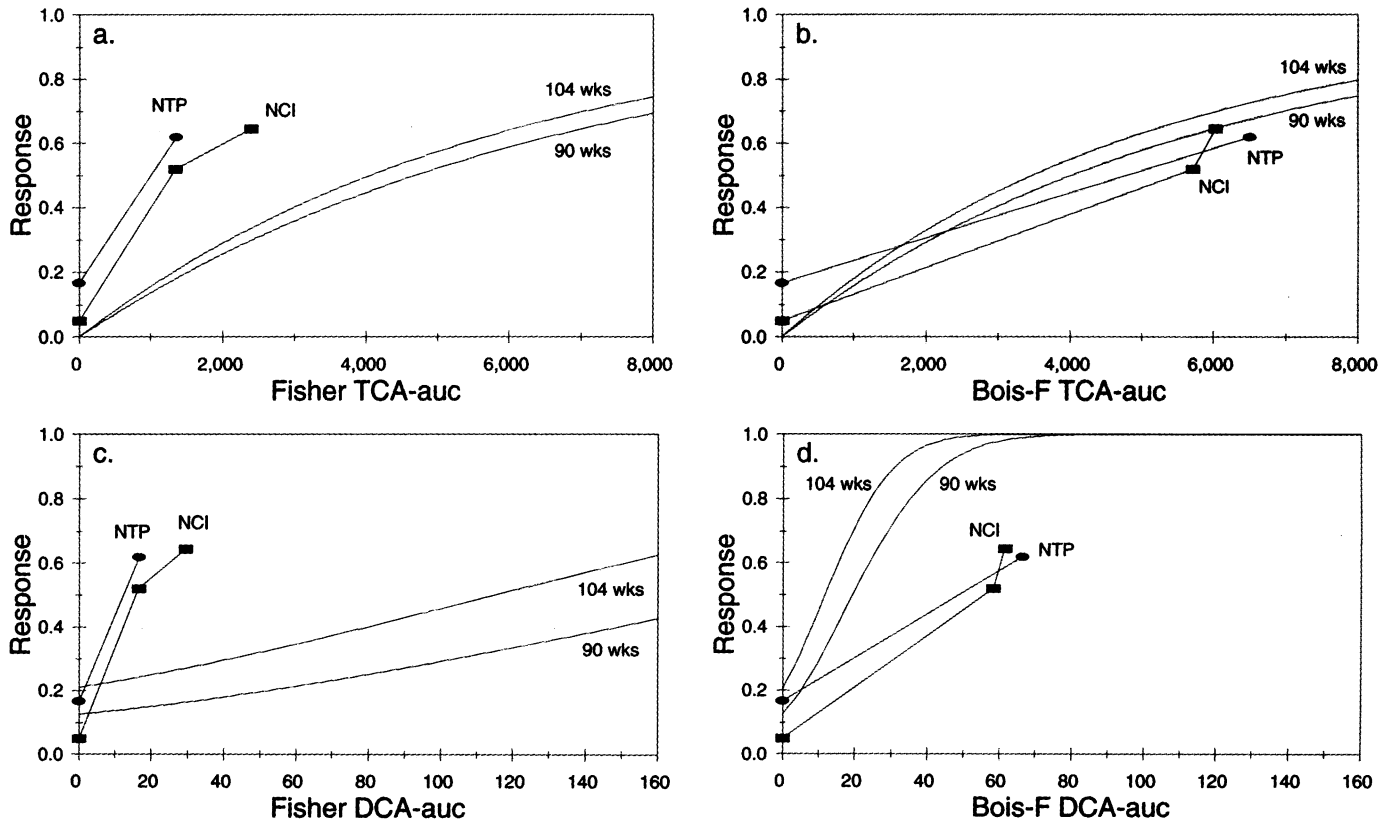

Figure 2. Predictions of mouse liver tumor response for 90-week and 104-week exposure (smooth curves) based on a dose-time–response model fitted to TCA and DCA drinking water bioassays together with mouse liver tumor responses observed in the NTP (*4*) and NCI (*40*) gavage studies of TCE (points), all plotted as a function of various internal dose measures: (*a*) Fisher (*9*) estimates of TCA–auc; (*b*) Bois (*30*) estimates of TCA–auc based on the Fisher model; (*c*) Fisher (*9*) estimates of DCA–auc; (*d*) Bois (*30*) estimates of DCA–auc based on the Fisher model.

lower than those based on liver or kidney tumors and since lung tumors only appeared in experiments when TCE was encountered by inhalation. It is also of interest that the projected human inhalation risks by the linear method from mouse liver tumors are greater than those calculated above for lung, and those from rat kidney tumor data are at least roughly comparable. For both rat kidney tumors and mouse liver tumors, inhalation experiments did show some response in the experimental animals, albeit not as marked as from gavage administration.

Rat Kidney Tumors

The toxicity and carcinogenicity of TCE to the kidney is reviewed by Lash et al. (*19*). TCE causes a low incidence of renal tubular cell adenomas and carcinomas in rats exposed via corn oil gavage (*3,4*). Although the tumors are few, this is a repeatable finding (Tables 10 and 11). Such tumors are historically rare in rats (0.4% among corn oil gavage controls), and their appearance among dosed animals is seen as biologically significant. Maltoni et al. (*22*) observed similar tumors in Sprague-Dawley rats exposed to TCE by inhalation, although Fukuda (*37*) found no renal tumors in female Sprague-Dawley rats exposed to up to 425 ppm. The rat tumor incidence data are tabulated in Tables 10 and 11.

TCE does not appear to cause kidney tumors in either mice or hamsters. In particular, the extensive bioassay testing of mice has not revealed any increase in kidney tumors, despite the fact that mice produce as much if not more of the key conjugative TCE metabolite implicated for renal toxicity, *S*-(1,2-dichlorovinyl)-L-cysteine (DCVC), and they have as much chronic kidney toxicity in lifetime bioassays as do rats. Although several epidemiologic studies show no effect, one study found increased kidney cancer in a retrospective study of cardboard factory workers (*45*). Wartenberg et al. (*38*) review the increasing evidence for association of TCE and human kidney cancer.

Although questions remain, it is generally felt that toxic effects in the kidney are caused by the reactive products of the further metabolism in the kidney of the products of the conjugative metabolism of TCE by the liver. Specifically, the metabolite DCVC can either be detoxified by formation of an *N*-acetyl derivative or it can produce a highly reactive thiol, *S*-(1,2-dichlorovinyl)thiol (DCVSH) as a result of DCVC metabolism in the kidney mediated by β-lyase (*19*). These reactions are known to take place in mice, rats, and humans, although the quantitative extent of their relative activity is difficult to characterize (*19*). The thiol appears to be able to cause a number of immediate toxic effects, including alkylation of DNA and proteins, oxidative stress, and mitochondrial dysfunction, which in turn lead to genotoxicity, cytotoxicity, and altered gene expression in renal tubular cells (*19*). In some combination, these effects in turn lead to the observed acute toxicity, chronic toxicity, and tumorigenicity of TCE in the kidney. According to current evidence, it does not appear that either the induction of peroxisome proliferation or the syndrome of $\alpha_2\mu$-globulin protein-droplet nephropathy, mechanisms that have been proposed as

Table 8. Mouse lung tumor incidences and doses.

Bioassay	Sex/strain	LADE, μg/m³	LADD, mg/kg/day	Malignant	Benign + malignant	CH–auc doses Clewell	CH–auc doses Bois-C	CH–max doses Clewell	CH–max doses Bois-C
Fukuda et al. (*37*)									
Inhalation (ppm), 107 weeks, 7 hr/day, 5 days/week									
0	Females	0	0	1/49	6/49	0	0	0	0
50	ICR mice	56,000	99	3/50	5/50	0.8	0.95	0.20	0.14
150		168,000	297	8/50	13/50	2.4	2.85	0.45	0.41
450		504,000	889	6/46	11/46	7.9	8.60	1.6	1.20
Maltoni et al. (*22*)									
Inhalation (ppm), 78 weeks, 7 hr/day, 5 days/week, followed until death									
0	Males	0	0	10/90		0	0	0	0
100	Swiss mice	84,000	148	11/90		1.2	1.43	0.3	0.27
300	(BT305)	252,000	445	23/90		3.7	4.35	1.0	0.82
600		504,000	889	27/90		9.4	8.25	2.6	1.50
0	Females	0	0	15/90		0	0	0	0
100	Swiss mice	84,000	148	15/90		1.2	1.43	0.3	0.27
300	(BT305)	252,000	445	13/90		3.7	4.35	1.0	0.82
600		504,000	889	20/90		9.4	8.25	2.6	1.50
0	Males	0	0	2/90		0	0	0	0
100	$B6C3F_1$ mice	84,000	148	2/90		1.2	1.43	0.3	0.27
300	(BT306)	252,000	445	3/90		3.7	4.35	1.0	0.82
600		504,000	889	1/90		9.4	8.25	2.6	1.50
0	Females	0	0	4/90		0	0	0	0
100	$B6C3F_1$ mice	84,000	148	6/90		1.2	1.43	0.3	0.27
300	(BT306)	252,000	445	7/90		3.7	4.35	1.0	0.82
600		504,000	889	15/90		9.4	8.25	2.6	1.50
0	Males	0	0	16/90		0	0	0	0
100	$B6C3F_1$ mice	84,000	148	9/90		1.2	1.43	0.3	0.27
300	(BT306bis)	252,000	445	12/90		3.7	4.35	1.0	0.82
600		504,000	889	9/90		9.4	8.25	2.6	1.50

Abbreviations: LADD, lifetime average daily dose; LADE, lifetime average daily exposure."Benign" tumors are adenomas; "Malignant" tumors are adenocarcinomas for Fukuda et al. (*37*); and "pulmonary tumors" are for Maltoni et al. (*22*). Pharmacokinetic models were not modified for different strains and sexes. Clewell et al. (*6*) provided no internal dose estimates for 150 ppm; therefore his 100-ppm value was multiplied by 1.5. Bois (*29*) did not allow for 78 weeks of exposure, so his estimates for CH–auc were multiplied by 78/104.

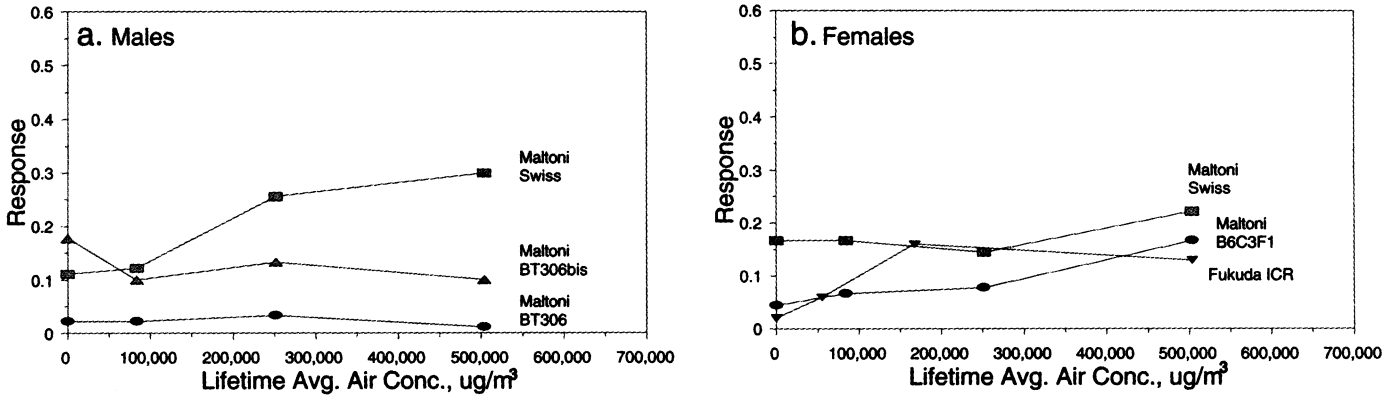

Figure 3. Mouse lung tumor responses from TCE inhalation bioassays (Table 8) plotted as a function of lifetime average air concentration: (*a*) males; (*b*) females.

Table 9. Linear method estimates of human incremental risk per μg/m³ of TCE in ambient air based on mouse lung tumors.

Data set	Dose metric: LADE, μg/m³	CH–auc, (mg-hr)/L: Clewell	CH–auc, (mg-hr)/L: Bois-C	CH–max, mg/L: Bois-C
Based on ED_{10} values				
Fukuda et al. (*37*)				
ICR females, adenocarcinomas	2.9×10^{-7}	6.6×10^{-9}	4.1×10^{-9}	1.3×10^{-9}
ICR females, adenomas + adenocarcinomas	3.5×10^{-7}	8.0×10^{-9}	4.9×10^{-9}	1.5×10^{-9}
Maltoni et al. (*22*)				
Swiss males, pulmonary tumors	5.1×10^{-7}	1.0×10^{-8}	7.5×10^{-9}	1.7×10^{-9}
Swiss females, pulmonary tumors	1.9×10^{-7}	3.8×10^{-9}	2.8×10^{-9}	6.5×10^{-10}
B6C3F1 males, pulmonary tumors (BT306)	2.1×10^{-7}	4.4×10^{-9}	3.1×10^{-9}	7.3×10^{-10}
Based on LED_{10} values				
Fukuda et al. (*37*)				
ICR females, adenocarcinomas	5.7×10^{-7}	1.4×10^{-8}	8.1×10^{-9}	2.5×10^{-9}
ICR females, adenomas + adenocarcinomas	7.1×10^{-7}	1.7×10^{-8}	1.0×10^{-8}	3.0×10^{-9}
Maltoni et al. (*22*)				
Swiss males, pulmonary tumors	7.5×10^{-7}	1.6×10^{-8}	1.1×10^{-8}	2.5×10^{-9}
Swiss females, pulmonary tumors	2.8×10^{-7}	6.1×10^{-9}	4.0×10^{-9}	9.2×10^{-10}
B6C3F$_1$ males, pulmonary tumors (BT306)	3.6×10^{-7}	7.9×10^{-9}	5.2×10^{-9}	1.2×10^{-9}

Clewell et al. (*6*) provide no CH–max estimate for humans. Bois (*29*) estimated human CH–max = 5.5×10^{-5} mg/L during 1 ppm inhalation.

Table 10. Rat kidney tumor incidences and doses.

Bioassay	Sex/strain	LADD, mg/kg/day	LADE, μg/m³	Malignant	Benign + malignant	Thiol doses: Clewell	Thiol doses: Bois-C
NTP (*4*)							
Gavage, 7 days/week, 104 weeks							
Untreated control	Males	0		0/49		0	0
Corn oil control	F344	0		0/48	0/48	0	0
500 mg/kg/day		357		0/49	2/49	32	2,800
1,000 mg/kg/day		714		3/49	3/49	73.6	7,700
Untreated control	Females	0		0/49		0	0
Corn oil control	F344	0		0/50	0/50	0	0
500 mg/kg/d		357		0/49	0/49	32	2,800
1,000 mg/kg/d		714		1/48	1/48	73.6	7,700
Maltoni et al. (*22*)							
Inhalation, 7 hr/day, 5 days/week, 104 weeks, ppm							
0	Males	0	0	0/135		0	0
100	Sprague-Dawley	95	112,000	0/130		0.31	57
300		238	336,000	0/130		8.4	990
600		567	672,000	4/130		26.1	4,200

"Malignant" tumors are renal tubular cell adenocarcinomas; "benign" tumors are adenomas. Clewell (*6*) estimates from his Table 7 are multiplied by 104/78 to account for 104-week rather than 78-week duration of the Maltoni et al. (*22*) experiment on rats. Bois-C doses from Bois (*30*).

Table 11. Kidney tumors from NTP multistrain gavage study of rats.

	Sex/strain	Renal tubular cell adenocarcinomas: Untreated controls	Vehicle controls	500 mg/kg/day	1,000 mg/kg/day
Males	ACI	0/49	0/50	1/49	0/49
	August	0/50	0/50	1/50	0/49
	Marshall	0/49	0/49	0/50	1/47
	Osborne-Mendel	0/50	0/50	0/50	1/50
	F344/N	0/49	0/48	0/49	3/49
	Male total	0/247	0/247	2/248	5/244
Females	ACI	0/49	0/48	1/47	1/43
	August	0/50	0/49	2/48	0/50
	Marshall	0/49	0/50	1/48	1/44
	Osborne-Mendel	0/50	0/50	0/50	0/49
	F344/N	0/49	0/50	0/49	1/48
	Female total	0/247	0/247	4/242	3/234
	All	0/494	0/494	6/490	8/478

NTP (*3*) declared this study to be "inadequate" because of problems in data reporting. The results are presented here for comparison to the outcomes of the NTP (*4*) study on F344 rats, which are also tabulated. "Malignant" tumors are renal tubular cell adenocarcinomas; "benign" tumors are adenomas. Clewell (*6*) estimates from his Table 7 are multiplied by 104/78 to account for 104-week rather than 78-week duration of the Maltoni et al. (*22*) experiment on rats. Bois-C doses from Bois (*30*).

causes of rat kidney tumors, are operative in the case of TCE (*19*).

Clewell et al. (*6*) and Bois (*29*) in his reanalysis of the Clewell pharmacokinetic model have produced estimates of the reactive thiol production in rat and human kidneys at relevant dose levels (Table 10), and these are used in the following quantitative analysis. The Clewell and Bois-C estimates are quite different, almost exactly 100-fold different. The reason for this discrepancy is not apparent without detailed examination of the models. The wide discrepancy is repeated in the human kidney thiol dose estimates (Table 3) and so the relative doses in rats and humans—the key to the impact on TCE carcinogenicity projection—are similar for the Clewell and Bois estimates. It is also of interest to note that the thiol doses estimated for the inhalation exposures of the Maltoni et al. (*22*) study evince a good deal of nonlinearity with exposure level.

The key data for rat kidney tumors are those from the male F344 rats in the 1990 NTP gavage bioassay (*4*) (Table 10). With only three adenocarcinomas, however, the role of statistical fluctuation in response can be appreciable, and little information can be gleaned about dose–response shape. To aid in interpretation, data are examined from a 1988 NTP gavage study on four additional strains of rats (*3*) (Table 11) conducted according to the same protocol as the 1990 study. It should be noted that the NTP declared this study to be "inadequate" due to problems in data reporting and because of some early mortality. These data are examined here for comparison with the analysis of the 1990 F344 rat study and to provide perspective on the shape of the dose–response relationship. The 1990 F344 rat study should be emphasized in drawing conclusions, however.

Although no adenocarcinomas occurred among 494 controls (including all 5 rat strains of both sexes), all experiments (excepting female Osborne-Mendel rats) had at least one such tumor among the dosed animals. Although responses are uniformly low (and they fluctuate accordingly), there is no marked difference among sexes or strains, and the pattern of low-frequency induction of the kidney tumors appears repeatable among the data sets, showing, in the aggregate, no tendency toward nonlinearity in the observed range.

Dose–Response Analysis

The standard reliance on 10% extra risk to define the PoD appears inappropriate for rat kidney tumors. This point is above rather than below all the observations, and (on the evidence of Table 11) an ongoing gradual drop in risk with decreasing dose is continuing in the range of 1–10% risk. Accordingly, for the analysis of the rat kidney tumors, an

alternative PoD based on 1% extra risk, i.e., on the ED_{01} and LED_{01}, is employed.

Although time-to-tumor data are available, the low number of responses makes it statistically difficult for the program MULTIWEIB (*23*) to converge to stable estimates, so multistage models fit with GLOBAL86 (*25*) were employed. (Time-to-tumor analysis for male F344 rats bearing both adenomas and adenocarcinomas yielded ED_{10} and LED_{10} values about half as great as the multistage model.) The resulting PoD doses are listed in Table 12.

The unit risks resulting from applying the U.S. EPA linear dose–response method to these values are shown in Tables 13 and 14. (Incremental risks per μg/L of contaminated drinking water can be obtained by dividing the entries of Table 13 by 35,000.) As administered dose defaults, the gavage doses use $mg/kg^{3/4}$/day scaling of intake, while the inhalation data are projected to humans on the basis of equal risk per $\mu g/m^3$ of air concentration. As discussed in "Methods" (under "Cross-Species Equivalency of Doses"), two approaches have been used regarding how to project risks across species on the basis of amounts of metabolites generated in target tissues: to assume equal carcinogenic effect from equal lifetime average daily production per unit of tissue, and to assume equal effect when daily production is proportional to the 3/4-power of body mass. These are the internal dose versions of the external-dose alternative scaling methods commonly termed body-weight scaling and surface-area scaling, respectively. The issues surrounding cross-species dose scaling for internal and external doses have been extensively discussed elsewhere (*26–28,32–36,41*). For the present article, it is sufficient to present the consequences of both approaches. Following prior U.S. EPA practice (*32,33*), the unit risk values tabulated in Tables 13 and 14 are calculated on the assumption that daily production of reactive thiol in the kidney gives equal risk in humans and rats when amounts are in proportion to the 3/4-power of body weight. [In practice, this is calculated by presuming that doses based on daily milligrams of thiol per gram of kidney are riskier in humans by a factor equal to the 4th root of the ratio of human to rat body weights, yielding unit risks that are $(70/0.35)^{1/4}$ or 3.76-fold higher than those obtained without this scaling assumption.] Projections based on equivalence of milligrams of thiol produced daily per gram of kidney (the body-weight scaling alternative) can be obtained by dividing the tabulated values by 3.76. That is, under this view, low-dose potencies are estimated to be 3.76-fold lower than shown in the thiol-dose columns of Tables 13 and 14.

The results show that there does not seem to be a pronounced difference in the carcinogenic potency in rat kidney between inhalation and gavage administration of TCE. The results based on the pooled data over five strains and both sexes of rats do not differ much from those based on the male F344 rats (*4*). The human incremental risk projections from rat kidney tumors are generally lower by one to three orders of magnitude than those from the analysis of mouse liver tumors.

Impact of Uncertainty in Internal Doses

Aside from the evident dependence of the calculations on which particular source of pharmacokinetic internal dose estimation is employed, the projections based on each source are uncertain because the physiological parameters embodied in the model are themselves not known with absolute precision. Bois (*29*) has conducted a Bayesian uncertainty analysis of the Clewell et al. (*6*) pharmacokinetic model, as previously described, and the results of this analysis yield approximately log-normal distributions for estimates of the internal dose measures that result from specific exposure scenarios. It is the median of each such distribution that is used above as one of the Bois-C internal dose estimates. Now the impact of the spread of these distributions, measured as the geometric standard deviation (GSD) will be considered.

It should be emphasized that this characterization of uncertainty is based solely on the impact of uncertainty about the values of the Clewell model physiological and metabolic parameters; it does not address questions about the mathematical structure of the model as a description of the underlying biological processes, the differences between the Clewell model and other models, or the appropriateness of the dose measures selected to describe relative cancer risk in animals and humans. Importantly, it also does not include estimates of the impact of variation among individual humans in rates of uptake and metabolic processing of TCE.

Bois (*29*) reports separate uncertainty distributions for each experimental exposure using an independent set of iterations that draw values for the various parameters from their respective uncertainty distributions. But since the animals are drawn from the same pool, the same true parameter values apply to all experimental groups, and the variations in estimated internal dose should be largely parallel among dose groups, shifting the entire curve of response versus internal dose up or down along the dose axis as parameters yielding higher or lower target-organ doses are considered. In practice, I use the uncertainty distribution of the internal dose at the lowest experimental exposure as an adequate approximation of the uncertainty in low internal-dose potency. The placement of the lowest response on the internal dose scale is the prime determinant of the ED_{10}, on which the dose–response analysis is based.

The human internal dose is also uncertain, and Bois (*29*) has estimated uncertainties in the dosimeter estimates for human environmental exposures as well. These tend to be larger than the animal uncertainties because of the more indirect means that are necessary for developing the human models.

The low-dose potency in humans (when projected from animals based on toxic equivalency of the internal dose) ultimately depends on the ratio of internal doses in animals and humans. Thus, the uncertainty

Table 12. LED_{01} and ED_{01} values based on rat kidney tumors.

Data set	Administered, mg/kg/day	LADE, $\mu g/m^3$	Kidney thiol dose, mg/L/day	
			Clewell	Bois-C
ED_{01} values				
NTP (*4*) gavage				
Males, adenocarcinomas	527		54.2	5,670
Males, adenomas + adenocarcinomas	103		10.1	1,005
NTP (*3,4*) 5 strains pooled				
Males, adenocarcinomas	422		39.0	3,663
Both sexes, adenocarcinomas	368		36.2	3,599
Maltoni et al. (*22*) inhalation				
Males, adenocarcinomas		558,000	21.6	3,477
LED_{01} values				
NTP (*4*) gavage				
Males, adenocarcinomas	123		11.3	1,030
Males, adenomas + adenocarcinomas	53		5.25	522
NTP (*3,4*) 5 strains pooled				
Males, adenocarcinomas	215		21.0	2,085
Both sexes, adenocarcinomas	244		24.1	2,389
Maltoni et al. (*22*) inhalation				
Males, adenocarcinomas		349,000	8.38	1,090

Based on multistage model of degree 2 for gavage studies and 3 for inhalation. Zero dose groups are vehicle controls. Multistage-Weibull analysis of NTP male adenomas + adenocarcinomas yields values about 1/2 as large. NTP (*3*) declared this study to be "inadequate" because of problems in data reporting. The results are presented here for comparison to the outcomes of the NTP (*4*) study on F344 rats, which are also tabulated. "Malignant" tumors are renal tubular cell adenocarcinomas; "benign" tumors are adenomas. Clewell (*6*) estimates from his Table 7 are multiplied by 104/78 to account for 104-week rather than 78-week duration of the Maltoni et al. (*22*) experiment on rats. Bois-C doses from Bois (*30*).

in this projection is the uncertainty in the ratio of two uncertain quantities, the uncertain internal dose values in animals and humans. The uncertainty in the product (or ratio) of two log-normal distributions H and A (for Human and Animal, with specified geometric standard deviations GSD_H and GSD_A) is itself a log-normal distribution with a GSD_{POT} (for potency) equal to

$$GSD_{POT} = \exp\sqrt{(\ln GSD_H)^2 + (\ln GSD_A)^2}.$$

Table 13. Linear method estimates of incremental risk per mg/kg/day of TCE intake based on rat kidney tumors.

Data set	Dose metric: mg/kg$^{3/4}$/day intake	Kidney thiol dose per kg$^{3/4}$: Clewell	Kidney thiol dose per kg$^{3/4}$: Bois-C
Based on ED_{01} values			
NTP (*4*) gavage			
Males, adenocarcinomas	7.1×10^{-5}	9.7×10^{-6}	1.4×10^{-6}
Males, adenomas + adenocarcinomas	3.7×10^{-4}	5.2×10^{-5}	7.9×10^{-6}
NTP (*3,4*), 5 strains pooled			
Males, adenocarcinomas	8.9×10^{-5}	1.4×10^{-5}	2.2×10^{-6}
Both sexes, adenocarcinomas	1.0×10^{-4}	1.5×10^{-5}	2.2×10^{-6}
Maltoni et al. (*22*) inhalation			
Males, adenocarcinomas		2.4×10^{-5}	2.3×10^{-6}
Based on LED_{01} values			
NTP (*4*) gavage			
Males, adenocarcinomas	3.1×10^{-4}	4.7×10^{-5}	7.7×10^{-6}
Males, adenomas + adenocarcinomas	7.1×10^{-4}	1.0×10^{-4}	1.5×10^{-5}
NTP (*3,4*) 5 strains pooled			
Males, adenocarcinomas	1.8×10^{-4}	2.5×10^{-5}	3.8×10^{-6}
Both sexes, adenocarcinomas	1.5×10^{-4}	2.2×10^{-5}	3.3×10^{-6}
Maltoni et al. (*22*) inhalation			
Males, adenocarcinomas		6.3×10^{-5}	7.2×10^{-6}

Unit incremental risks per μg/L of drinking water (assuming lifetime consumption of 2 L/day) may be obtained by dividing the tabled entries by 35,000. The tabled numbers for kidney thiol doses are based on adjusting the risk from a given daily mg thiol production per g of kidney by the 4th root of the ratio of rat to human body weight, i.e., by $(0.35/70)^{1/4}$. Projections not scaled by this factor (i.e., based on equivalent daily milligram thiol per gram of kidney) may be obtained by dividing the tabled numbers by 3.76. NTP (*3*) declared this study to be "inadequate" because of problems in data reporting. The results are presented here for comparison to the outcomes of the NTP (*4*) study on F344 rats, which are also tabulated. "Malignant" tumors are renal tubular cell adenocarcinomas; "benign" tumors are adenomas. Clewell (*6*) estimates from his Table 7 are multiplied by 104/78 to account for 104-week rather than 78-week duration of the Maltoni et al. (*22*) experiment on rats. Bois-C doses from Bois (*30*).

Table 14. Linear method estimates of incremental risk per μg/m^3 of TCE in ambient air.

Dataset	Dose metric: LADE, μg/m^3	mg/kg$^{3/4}$/day intake	Kidney thiol dose per kg$^{3/4}$: Clewell	Kidney thiol dose per kg$^{3/4}$: Bois-C
Based on ED_{01} values				
Gavage				
NTP (*4*)				
Males, adenocarcinomas		2.0×10^{-8}	1.0×10^{-9}	1.4×10^{-10}
Males, adenomas + adenocarcinomas		1.1×10^{-7}	5.6×10^{-9}	7.7×10^{-10}
NTP (*3,4*), 5 strains pooled				
Males, adenocarcinomas		2.6×10^{-8}	1.4×10^{-9}	2.1×10^{-10}
Both sexes, adenocarcinomas		2.9×10^{-8}	1.5×10^{-9}	2.1×10^{-10}
Inhalation				
Maltoni et al. (*22*)				
Males, adenocarcinomas	1.8×10^{-8}		2.6×10^{-9}	2.2×10^{-10}
Based on LED_{01} values				
Gavage				
NTP (*4*)				
Males, adenocarcinomas		8.7×10^{-8}	5.0×10^{-9}	7.5×10^{-10}
Males, adenomas + adenocarcinomas		2.0×10^{-7}	1.1×10^{-8}	1.5×10^{-9}
NTP (*3,4*), 5 strains pooled				
Males, adenocarcinomas		5.0×10^{-8}	2.7×10^{-9}	3.7×10^{-10}
Both sexes, adenocarcinomas		4.4×10^{-8}	2.3×10^{-9}	3.2×10^{-10}
Inhalation				
Maltoni et al. (*22*)				
Males, adenocarcinomas	2.9×10^{-8}		6.7×10^{-9}	7.1×10^{-10}

The table numbers for kidney thiol doses are based on adjusting the risk from a given daily milligram thiol production per gram of kidney by the 4th root of the ratio of rat to human body weight, i.e., by $(0.35/70)^{1/4}$. Projections not scaled by this factor (i.e., based on equivalent daily mg thiol per g of kidney) may be obtained by dividing the tabled numbers by 3.76. NTP (*3*) declared this study to be "inadequate" owing to problems in data reporting. The results are presented here for comparison to the outcomes of the NTP (*4*) study on F344 rats, which are also tabulated. "Malignant" tumors are renal tubular cell adenocarcinomas; "benign" tumors are adenomas. Clewell (*6*) estimates from his Table 7 are multiplied by 104/78 to account for 104-week rather than 78-week duration of the Maltoni et al. (*22*) experiment on rats. Bois-C doses from Bois (*30*).

Table 15 shows the application of this principle to extrapolations based on the Bois-C internal dose estimates. For a log-normal distribution, approximately 95% of the values are contained in the span defined by multiplying or dividing the geometric mean by the square of the GSD. It is evident from the approximate uncertainty propagation undertaken here that the human unit risks based on kidney cancer and the reactive thiol tissue doses are quite uncertain, being reasonably placed within a factor of 74 higher or lower than the central estimate. The projections of lung tumor risk based on CH production are yet more uncertain. The uncertainty in human risks based on analysis of mouse liver tumors and using either TCA or DCA as an internal dosimeter is moderate; the analysis implies a range of about a factor of 10 higher or lower.

Discussion and Conclusions

The foregoing analyses have provided a large number of potential bases for an estimate of the carcinogenic potency of TCE in humans. The aim has been to examine the alternative approaches and to explore the consequences of assumptions and methodological choices. The alternatives are not all equally compelling; the present article has laid out an array of analytical paths for further careful interpretation in the context of our knowledge of the biological processes underlying the disposition of TCE in the body and toxic actions in the tissues. A second objective of the present article is to examine the patterns of dose and tumor response for evidence bearing on nonlinear modes of carcinogenic action. Ultimately, the decision to follow the linear or nonlinear approach in the proposed new U.S. EPA guidelines (*10*) depends on understanding of underlying biological mechanisms, but information on nonlinear behavior in the range of observable tumor response can inform the interpretation and judgments of such mechanistic data.

The most recent U.S. EPA analysis of TCE potency (*2*) recommended a unit risk for lifetime inhalation of contaminated air of 1.7×10^{-6} per μg/m^3 on the basis of mouse lung tumors and an estimate of the fraction of inhaled TCE that is metabolized. Some of the linear method analyses presented herein based on administered dose suggest a similar, although in some cases slightly higher, value. [The most sensitive administered dose basis, for example, is that for combined liver adenomas and adenocarcinomas in male mice from the NTP (*4*) gavage bioassay (Table 6), which lead to an estimated inhalation unit risk of 8.9×10^{-6} per μg/m^3 if based on linear projection from the LED_{10}, a value 5.2-fold higher than the former number.] The difference is due to several factors, including the use of different animal data and tumor responses, the use of time-to-tumor methods

to allow for intercurrent mortality, and the slight differences in default methodology between the 1986 and 1996 U.S. EPA guidelines.

The major change since the previous U.S. EPA analysis, however, is the advent of pharmacokinetic models that estimate the target-tissue exposures of key metabolites thought to be responsible for the carcinogenic actions of TCE in animals. These models are evolving, and a major task of the present article is to examine their potential consequences as currently formulated, recognizing that internal dose estimation will improve with further work.

The most striking conclusion is that the alternative models sometimes estimate substantially different values for internal doses corresponding to exposure regimes of interest to the risk analysis. Patterns of nonlinearity of metabolic activity and relative internal doses arising from different routes of administration can also differ substantially among model implementations. The fact that the Bayesian updating conducted by Bois (*29,30*), which is based on assessment of the performance of the models in simulating data on pharmacokinetic outcomes, can substantially alter model characteristics and predictions is cause for concern regarding the robustness of estimation of key metabolic parameters.

The immediate consequence of these differences is that it is necessary to run a number of parallel analyses using the different estimates from each model. This makes it difficult to draw firm conclusions when phenomena of interest are inconsistent among models. For instance, the question of whether metabolically generated TCA or DCA can account for the mouse liver tumors observed from TCE gavage is difficult to address, since the compatibility of outcomes of TCA and DCA drinking water bioassays with the TCE gavage assays depends on which set of internal dose estimates is being considered.

In view of these differences among models, it is perhaps surprising that employing internal dosimeters in the risk analysis does not make more difference to the final outcome. Although there are some substantial impacts (and model-dependent differences in impacts) to consider, the differences among models in description of animal and human pharmacokinetics tend to vary in parallel, and they are often in approximate agreement regarding projected human risks.

Nonlinear pharmacokinetics are most pronounced in the activity of the oxidative pathway in mouse gavage studies in which liver tumors were observed, and the pattern is in the direction of less efficient generation of TCA and DCA at bioassay doses than at lower exposure levels. The effect on high-to-low–dose extrapolation (all else being equal) is to raise the risk associated with lower doses compared to an administered dose analysis that does not account for this nonlinearity. Within the range of observation of rat kidney tumors, there is evidence of substantial nonlinearity of reactive thiol production. This is of the opposite pattern, with higher doses yielding proportionally more thiol exposure to the kidneys. To the extent that this nonlinearity extends below the observed range, it will tend to render lower exposures less risky, and the low estimates of human risk projected from rat kidney tumors on the basis of thiol doses are in part a reflection of this.

The second aspect of the impact of internal dosimetry is that of differences between experimental animals and humans in the relative internal doses produced by TCE exposures. Interpretation of these results is hampered by uncertainty regarding the levels of internal dose that are expected to be equally carcinogenic in different species, and the results presented here are contingent on the assumptions about such equivalence. To a large degree, the pharmacokinetic analyses show humans and animals not to be radically different in internal dose levels for a given administered amount of TCE. Human risk projections based on mouse liver tumors and either TCA–auc or DCA–auc as a dose measure tend to lead to higher risk levels by a few fold, reflecting that humans have as high or higher areas-under-the-curve or these stable metabolites than mice after similar exposures. For instance, the linear method inhalation unit risk based on the male mouse liver adenomas and adenocarcinomas, when based on the Fisher estimates of TCA–auc, is 5.8×10^{-5} per $\mu g/m^3$, which is 6.5-fold higher than that based on administered doses, while that based on the Clewell TCA–auc estimates is 1.6×10^{-4} per $\mu g/m^3$, or 18-fold higher than that based on administered dose (Table 6). On the other hand, projections of liver tumor risk based on DCA–auc are similar to or slightly lower than those based on administered dose; that based on the Clewell DCA–auc estimates is 1.0×10^{-6} per $\mu g/m^3$, nearly an order of magnitude less.

Examination of the dose–response curves with respect to TCA and DCA attempts to compare bioassays by similar and different routes of administration, and consideration of the apparent potency of TCA and DCA when administered to mice all failed to provide a basis for preferring one metabolite over the other as a basis for the mouse liver tumors. This matter will have to be addressed on mechanistic grounds (*16*). On the other hand, the analysis shows that, at least according to current pharmacokinetic modeling of these metabolites, the choice makes relatively little practical difference in the ultimate risk estimation, as TCA and DCA levels are highly correlated with one another. Changes in the view of the relative amounts of these metabolites produced in humans would have considerable potential impact however. Interpretation of the projection of mouse liver tumor risk to humans should be

Table 15. Approximate uncertainty analysis based on log-normal error.

	Uncertainty in potencies based on the Bois (*29*) internal dose estimates (Bois-C estimates)		
Human potency based on	Uncertainty in animal internal dose, GSD_A	Uncertainty in human internal dose, GSD_H	Uncertainty in human potency, GSD_{POT}
Mouse liver, TCA–auc	2.1	2.4	3.2
Mouse liver, DCA–auc	2.7	2.2	3.6
Rat kidney, thiol	3.4	6.2	9.0
Mouse lung, CH–auc	3	9	11.7
Mouse lung, CH–max	3.5	9	12.5

	Factor different from median estimate										
	Percentile of potency uncertainty distribution										
Human potency based on	1	2.5	5	10	25	50	75	90	95	97.5	99
Mouse liver, TCA–auc	1/15	1/10	1/7	1/4.4	1/2.2	1	2.2	4.4	7	10	15
Mouse liver, DCA–auc	1/20	1/12	1/8	1/5	1/2.4	1	5	5	8	12	20
Rat kidney, thiol	1/170	1/74	1/37	1/17	1/4.4	1	4.4	17	37	74	170
Mouse lung, CH–auc	1/300	1/120	1/56	1/23	1/5.2	1	5.2	23	56	120	300
Mouse lung, CH–max	1/360	140	1/63	1/25	1/5.4	1	5.4	25	63	140	360

See text for additional information.

tempered by the dependence on source of pharmacokinetic doses and on the analysis of uncertainty within models described in Table 15. As with all risk analyses based on target-organ doses, the projection to humans implicitly assumes cross-species site concordance, an assumption that has proven to have limited utility in carcinogen risk assessment.

It is the projection to humans of mouse liver tumor risks, however, that poses the most concern. The projected risk levels are higher than those from the mouse lung or rat kidney tumors, and the added consideration of internal dosimetry tends to raise the risk projections for mouse liver tumors while lowering them (by an order of magnitude or more) for the mouse lung and rat kidney tumors. One must note the uncertainty in the impact of internal dosimetry for the lung and kidney tumors, however (Table 15). Moreover, if a nonlinear approach is taken to the liver tumors but not to the rat kidney tumors (on the grounds of genotoxicity of DCVC), then the relative importance to low human doses could change.

It may appear that the analysis herein focuses on the EPA linear method of dose–response analysis, but in fact both the linear and nonlinear methods, when based on observations of tumor risk, share the same PoD, and the calculations herein of ED_{10} values can be used to determine margins of exposures against 10% elevation in tumor risk as well as for linear low-dose extrapolation. It is more accurate to say that the emphasis has been on analysis of the observations regarding tumor response, while questions of underlying mechanisms, their potential nonlinearity in dose–response patterns, and the determination of dose levels associated with precursor biological responses that may be without appreciable effect on secondary carcinogenesis are not considered. These important questions must be addressed in a full risk analysis of TCE carcinogenicity, however, of which the present article addresses only one aspect.

Nonetheless, the rationale behind the nonlinear method is that certain underlying mechanisms should generate steep dose–response curves and that a "break" between dose ranges that are acting to elevate cancer risk and those that are not can be identified. The steepness of the dose–response curve in the observable range is among the criteria used in determining the size of the acceptable Margin of Exposure (*10*). It is noteworthy, then, that the observable parts of the dose–response relationships for the tumors engendered in experimental animals by TCE exposure show little sign of nonlinearity and evince little basis to identify dose ranges in which basic shifts in underlying biological processes are at work. Any invocation of nonlinearity in the TCE tumor responses, and any identification of the dose levels at which mechanisms operate at a level insufficient to raise carcinogenicity concerns will have to be based on studies of mechanisms of carcinogenic action, and such points will fall somewhere below the range that is observed in current animal bioassays. From this point of view, it is unfortunate that the mouse liver tumor studies, which are key to estimates of human risk, include only rather high doses with high responses and lack the series of doses that would allow better characterization of the shape of this critical dose–response curve.

References and Notes

1. U.S. EPA. Health Assessment Document for Trichloroethylene. Final Report. EPA/600/8-82/006F. Washington, DC:U.S. Environmental Protection Agency, 1985.
2. U.S. EPA. Addendum to the Health Assessment Document for Trichloroethylene: Updated Carcinogenicity Assessment for Trichloroethylene. External Review Draft EPA/600/8-82/006FA. Washington, DC:U.S. Environmental Protection Agency, 1987.
3. NTP. NTP Technical Report on the Toxicology and Carcinogenesis Studies of Trichloroethylene (CAS No. 79-01-6) in Four Strains of Rats (ACI, August, Marshall, Osborne-Mendel) (Gavage Studies). NTP TR 273. Research Triangle Park, NC: National Toxicology Program, 1988.
4. NTP. Carcinogenesis Studies of Trichloroethylene (Without Epichlorohydrin) (CAS No. 79-01-6) in F344/N Rats and $B6C3F_1$ Mice (Gavage Studies). NTP TR 243. Research Triangle Park, NC:National Toxicology Program, 1990.
5. Allen BC, Fisher JW. Pharmacokinetic modeling of trichloroethylene and trichloroacetic acid in humans. Risk Anal 13:71–86 (1993).
6. Clewell HJ III, Gentry PR, Covington TR, Gearhart JM. Development of a physiologically based pharmacokinetic model of trichloroethylene and its metabolites for use in risk assessment. Environ Health Perspect 108(suppl 2):283–305 (2000).
7. Clewell HJ III, Gentry PR, Gearhart JM, Allen BC, Andersen ME. Considering pharmacokinetic and mechanistic information in cancer risk assessments for environmental contaminants: examples with vinyl chloride and trichloroethylene. Chemosphere 31:2561–2578 (1995).
8. Fisher JW, Allen BC. Evaluating the risk of liver cancer in humans exposed to trichloroethylene using physiological models. Risk Anal 13:87–95 (1993).
9. Fisher JW. Physiologically based pharmacokinetic models for trichloroethylene and its oxidative metabolites. Environ Health Perspect 108(suppl 2):265–273 (2000).
10. U.S. EPA. Proposed Guidelines for Carcinogen Risk Assessment. EPA/600/P-92/003C. Washington, DC:U.S. Environmental Protection Agency, 1996.
11. Bull RJ, Sanchez IM, Nelson MA, Larson JL, Lansing AJ. Liver tumor induction in $B6C3F_1$ mice by dichloroacetate and trichloroacetate. Toxicology 63:341–359 (1990).
12. Daniel FB, DeAngelo AB, Stober JA, Olson GR, Page NP. Hepatocarcinogenicity of chloral hydrate, 2-chloroacetaldehyde, and dichloroacetic acid in the male $B6C3F_1$ mouse. Fundam Appl Toxicol 19:159–168 (1992).
13. DeAngelo AB, Daniel FB, Stober JA, Olson GR. The carcinogenicity of dichloroacetic acid in the male $B6C3F_1$ mouse. Fundam Appl Toxicol 16:337–347 (1991).
14. Herren-Freund SL, Pereira MA, Khoury MD, Olson G. The carcinogenicity of trichloroethylene and its metabolites, trichloroacetic acid and dichloroacetic acid, in mouse liver. Toxicol Appl Pharmacol 90:183–189 (1987).
15. Pereira MA. Carcinogenic activity of dichloroacetic acid and trichloroacetic acid in the liver of female $B6C3F_1$ mice. Fundam Appl Toxicol 31:192–199 (1996).
16. Bull RJ. Mode of action of liver tumor induction by trichloroethylene and its metabolites, trichloroacetate and dichloroacetate. Environ Health Perspect 108(suppl 2):214–259 (2000).
17. Green T. The pulmonary toxicity and carcinogenicity of trichloroethylene: species differences and modes of action. Environ Health Perspect 108(suppl 2):261–264 (2000).
18. Lash LH, Fisher JW, Lipscomb J, Parker JC. Metabolism of trichloroethylene. Environ Health Perspect 108(suppl 2):177–200 (2000).
19. Lash LH, Parker JC, Siegel Scott C. Modes of action of trichloroethylene for kidney tumorigenesis. Environ Health Perspect 108(suppl 2):255–240 (2000).
20. Barton HA, Clewell HJ III. Evaluating noncancer effects of trichloroethylene: dosimetry, mode of action, and risk assessment. Environ Health Perspect 108(suppl 2):323–334 (2000).
21. Henschler D, Romen W, Elasser HM, Reichert D, Eder E, Radwan Z. Carcinogenicity study of trichloroethylene by longterm inhalation in three animal species. Arch Toxikol 43:237–248 (1980).
22. Maltoni C, Lefemine G, Cotti G, Perino G. Long-term carcinogenicity bioassays on trichloroethylene administered by inhalation to Sprague-Dawley rats and Swiss and $B6C3F_1$ mice. Ann NY Acad Sci 534:316–342 (1986).
23. Howe RB, Crump KS. MULTI-WEIB: A Computer Program to Extrapolate Time to Tumor Animal Toxicity Data to Low Doses. Ruston, LA:Clement Associates, 1991.
24. Krewski D, Crump K, Farmer J, Gaylor D, Howe R, Portier C, Salsburg D, Sielken R, Van Ryzin J. A comparison of statistical methods for low dose extrapolation utilizing time-to-tumor data. Fundam Appl Toxicol 3:140–158 (1983).
25. Howe RB, Crump KS, Van Landingham C. GLOBAL86: A Computer Program to Extrapolate Quantal Animal Toxicity Data to Low Doses. Ruston, LA:K.S. Crump, 1986.
26. EPA. A cross-species scaling factor for carcinogen risk assessment based on equivalence of $mg/kg^{3/4}$/day. Fed Reg 57:42152–42173 (1992).
27. Rhomberg LR. What constitutes 'dose'? (Definitions). In: Low-Dose Extrapolation of Cancer Risk: Issues and Perspectives (Olin S, Farland W, Park C, Rhomberg L, Scheuplein R, Starr T, Wilson J, eds). Washington, DC:ILSI Press, 1995.
28. Rhomberg LR. Use of quantitative modelling in methylene chloride risk assessment. Toxicology 102:95–114(1995).
29. Bois FY. Statistical analysis of Clewell et al. PBPK model of trichloroethylene kinetics. Environ Health Perspect 108(suppl 2):307–316 (2000).
30. Bois FY. Statistical analysis of Fisher et al. PBPK model of trichloroethylene kinetics. Environ Health Perspect 108(suppl 2):275–282 (2000)..
31. U.S. EPA. Methods for Derivation of Inhalation Reference Concentrations and Application of Inhalation Dosimetry. EPA/600/8-90/066F. Washington, DC:U.S. Environmental Protection Agency, 1994.
32. U.S. EPA. Technical Analysis of New Methods and Data Regarding Dichloromethane Hazard Assessment. External Review Draft. EPA/600/8-87/029A. Washington, DC:U.S. Environmental Protection Agency, 1987.
33. U.S. EPA. Update to the Health Assessment Document and Addendum for Dichloromethane (Methylene Chloride): Pharmacokinetics, Mechanisms of Action, and Epidemiology. External Review Draft. EPA/600/8-87/030A. Washington, DC:U.S. Environmental Protection Agency, 1987.
34. Andersen ME, Clewell HJ III, Krishnan K. Tissue dosimetry, pharmacokinetic modeling, and interspecies scaling factors. Risk Anal 15:533–537 (1995).
35. Mordenti J. Man versus beast: pharmacokinetic scaling in mammals. J Pharmac Sci 75:1028–1040 (1986).
36. Travis CC, White RK, Ward RC. Interspecies extrapolation of pharmacokinetics. J Theoret Biol 142:285–304 (1990).
37. Fukuda K, Takemoto K, Tsuruta H. Inhalation carcinogenicity of trichloroethylene in mice and rats. Ind Health 21:243–254 (1983).
38. Wartenberg D, Reyner D, Scott CS. Trichloroethylene and cancer: epidemiologic evidence. Environ Health Perspect 108(suppl 2):161–176 (2000).
39. Moore M, Harrington-Brock K. Mutagenicity of trichloroethylene and its metabolites: implications for the risk assessment of trichloroethylene. Environ Health Perspect 108(suppl 2):215–2230 (2000).
40. NCI. Carcinogenesis Bioassay of Trichloroethylene. CAS No. 79-01-6 NIH-77-813. Bethesda, MD:National Cancer Institute, 1976.
41. Andersen ME, Clewell HJ III, Gargas ML, Smith FA, Reitz RH. Physiologically based pharmacokinetics and the risk assessment process for methylene chloride. Toxicol Appl Pharmacol 87:185–205 (1987).
42. Smith AE, Gray GM, Evans JS. The ability of predicted internal dose measures to reconcile tumor bioassay data for chloroform. Regul Toxicol Pharmacol 21:339–351 (1995).
43. Bell Z, Olson K, Benya T. Final Report of Audit Findings of the Manufacturing Chemists Association (MCA): Administered Trichloroethylene (TCE) Chronic Inhalation Study at Industrial Bio-Test Laboratorie, Decatur, IL:Bio-Test Laboratories, 1978.
44. Odum J, Foster JR, Green T. A mechanism for the development of Clara cell lesions in the mouse lung after exposure to trichloroethylene. Chem-Biol Interact 83:135–153 (1992).
45. Henschler D, Vamvakas S, Lammert M, Dekant W, Kraus B, Thomas B, Ulm K. Increased incidence of renal cell tumors in a cohort of cardboard workers exposed to trichloroethene. Arch Toxikol 69:291–299 (1995).